

REF
671.7
1995
ASM

**STUDY ON THE MECHANICAL PROPERTIES OF
ELECTROPLATED IRON-CARBON ALLOY COATING**

ASMA YASMIN

A thesis submitted to the Department of Metallurgical Engineering, Bangladesh University of Engineering and Technology, Dhaka, in partial fulfilment of the requirements for the degree of Master of Science in Engineering (Metallurgical)



October, 1995

**BANGLADESH UNIVERSITY OF ENGINEERING AND TECHNOLOGY
DHAKA, BANGLADESH**



DECLARATION

This is to certify that this research work has been carried out by the author under the supervision of Dr. A. S. M. A. Haseeb, Assistant Professor, Department of Metallurgical Engineering, BUET, Dhaka, and it has not been submitted elsewhere for the award of any other Degree or Diploma.

Countersigned



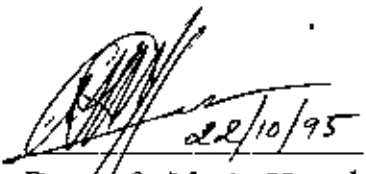
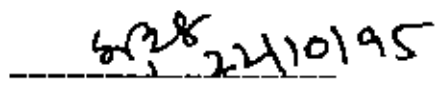
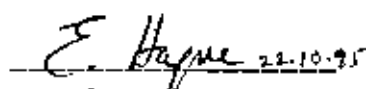
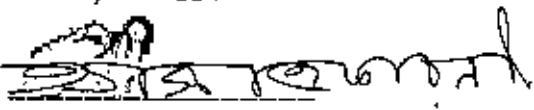
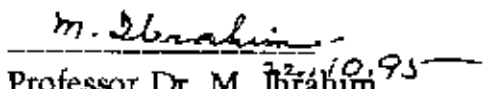
22/10/95

Supervisor

A. Yasmin
22.10.95

Signature of the author

The undersigned examiners appointed by the Committee of Advanced Studies and Research (CASR) hereby recommend to the Department of Metallurgical Engineering of Bangladesh University of Engineering and Technology, Dhaka, the acceptance of the thesis entitled **"STUDY ON THE MECHANICAL PROPERTIES OF ELECTROPLATED IRON-CARBON ALLOY COATING"** submitted by Asma Yasmin, B.Sc. Engg. (Metallurgical) in partial fulfilment of the requirements for the Degree of Master of Science in Engineering (Metallurgical)

1.  22/10/95
Dr. A. S. M. A. Haseeb
Assistant Professor
Dept. of Metallurgical Engg.
BUET, Dhaka. Chairman
(Supervisor)
2.  22/10/95
Head
Dept. of Metallurgical Engg.
BUET, Dhaka. Member
(ex-officio)
3.  22.10.95
Dr. Ehsanul Haque
Professor
Dept. of Metallurgical Engg.
BUET, Dhaka. Member
4.  22.10.95
Dr. A. S. W. Kurny
Professor
Dept. of Metallurgical Engg.
BUET, Dhaka. Member
5.  22/10/95
Professor Dr. M. Ibrahim
House No. 31, Road No. 4
Dhanmondi R/A, Dhaka. Member
(External)

ACKNOWLEDGEMENT

The author would like to express her gratitude and indebtedness to her thesis supervisor Dr. A. S. M. A. Haseeb, Assistant Professor, Department of Metallurgical Engineering, BUET, for his valuable suggestions, inspiring guidance, constant encouragement and kind help in carrying out the project and also in preparing this thesis.

The author is also indebted to Professor Md. Mohafizul Haque and Professor A. S. W. Kurny of the Department of Metallurgical Engg. for their inspiration and suggestions in completing this thesis.

The author would like to give thanks to Dr. A. K. M. Bazlur Rashid, Assistant Professor, Dept. Of Metallurgical Engg. for his kind help in preparing this thesis.

The author is grateful to Md. Ashikur Rahman, Laboratory Instructor, Md. Lutfur Rahman, Ex. Senior Crafts Instructor, Babu Binoy Bhushan Shaha, Senior Laboratory Instructor and other laboratory staff of Metallurgical Engg. Department of BUET for their kind help at different stages of this project.

Finally the author expresses her gratitude to her parents and well wishers for their encouragement and inspiration throughout the entire period of this undertaking.

Dept. of Metallurgical Engg.

BUET, Dhaka

The author

ABSTRACT

Electrodeposition of martensitic Fe-C and Fe-Ni-C alloy coatings was carried out from sulphate based baths at room temperature. The baths contained various amounts of citric acid (0.2 to 10 g/l) and L-Ascorbic acid (0.2 to 10 g/l) and in some cases additives viz. gelatin (0.2 to 1 g/l), sodium lauryl sulphate (0.5 g/l) to observe their influences on the morphology and mechanical properties of the coatings.

Chemical analysis showed the carbon content of both Fe-C and Fe-Ni-C alloy deposits to be above 1% and Ni content of Fe-Ni-C alloy deposit within 4-6%. It was observed that the carbon content of the Fe-C deposits becomes less sensitive to CA and LAA content of the bath as higher amounts of CA and LAA are added. Structure of the deposit was examined by optical microscopy and X-ray diffractometry. The microstructure of as-deposited etched sample was dark and difficult to observe under a microscope, but the annealed structure showed a structure similar to annealed carbon steel. X-ray diffraction pattern of as-deposited Fe-1.1%C alloys suggests these to be martensitic in structure.

Mechanical properties of these coatings viz. microhardness, ductility, wear resistance were investigated in relation to the presence of additives like gelatin and sodium lauryl sulphate in the bath and post-deposition heat treatment. Fe-C alloy deposited from bath containing 10 g/l CA and 10 g/l LAA showed hardness as high as 790 HV, whereas the deposits from other baths showed relatively lower hardness values such as 701, 386 HV. It was found that as the percentage of CA and LAA in the bath decreases, hardness of the deposit also decreases. Tempering of the as-deposited Fe-1.1%C alloy at 200°C for half an hour does not cause any appreciable decrease in hardness. However, gelatin was found to have a significant role on hardness; as the gelatin content in the bath increases, the corresponding hardness decreases. It was found that presence of gelatin in the baths and tempering of the deposits cause considerable improvement in ductility. Fe-4.3%Ni-1.1%C alloy showed better ductility than as deposited or tempered Fe-1.1%C alloy.

Wear tests were performed on both as-deposited and tempered Fe-1.1%C alloy coatings to evaluate their wear characteristics and then the values obtained were compared with the wear resistance of mild steel. Fe-1.1%C alloy coatings, in spite of their high hardness, showed lower wear resistance than mild steel probably due to their low toughness and insufficient adhesion.

CONTENTS

Acknowledgement

Abstract

	Page No.
1. INTRODUCTION	1
2. LITERATURE REVIEW	3
2.1 Electrodeposition of alloys	3
2.1.1 General conditions for electrodeposition of alloys	3
2.1.2 Principles of alloy deposition	4
2.1.3 Types of alloy plating systems	5
2.1.4 Effect of plating variables on the composition of the alloy deposit	7
2.1.4.1 Introduction	7
2.1.4.2 Concentration of depositable metals in the bath	8
2.1.4.3 Concentration of complexing agents in the bath	12
2.1.4.4 pH	13
2.1.4.5 Current density	15
2.1.4.6 Temperature	17
2.1.4.7 Bath agitation	18
2.1.4.8 Addition agents	19
2.2 Structure of electrodeposited alloys	21
2.3 Effect of heat treatment on microstructure	24
2.4 Structure of electrodeposited alloys as revealed by X-ray	25
2.5 Mechanical properties of electrodeposited alloys	27
2.5.1 Introduction	27
2.5.2 Hardness	28
2.5.3 Ductility	30
2.5.4 Wear resistance	32
2.6 Structure and properties of thermally prepared commercial iron-carbon based alloys	38

3. EXPERIMENTAL	46
3.1 Electroplating	46
3.1.1 Substrate and its pretreatment	46
3.1.2 Electroplating set-up	48
3.1.3 Preparation of Fe-C and Fe-Ni-C alloy coatings	49
3.2 Chemical analysis	50
3.3 Optical microscopy	51
3.4 X-ray diffraction	52
3.5 Differential thermal analysis	52
3.6 Mechanical properties	54
3.6.1 Microhardness measurement	54
3.6.2 Bend test	54
3.6.3 Wear test	55
4. RESULTS AND DISCUSSIONS	57
4.1 Characterization of Fe-C and Fe-Ni-C alloy coatings	57
4.1.1 Chemical composition	57
4.1.2 Structure and morphology	59
4.1.3 X-ray diffraction	63
4.1.4 Differential thermal analysis	65
4.2 Properties of Fe-C and Fe-Ni-C alloy coatings	67
4.2.1 Hardness	67
4.2.2 Ductility	70
4.2.3 Wear properties	73
5. CONCLUSIONS	81
6. SUGGESTIONS FOR FUTURE STUDY	82
7. REFERENCES	83



1. INTRODUCTION

Electrodeposited alloys possess many special, potential applications by virtue of their great range and diversity of properties. Certain alloys may be prepared more readily by electrodeposition than by thermal means. For example, the preparation of an alloy consisting of a low-melting volatile constituent and a metal with a high melting point may be difficult to prepare by conventional means and may be more easily achieved by electrodeposition. Alloys which form mechanical mixtures, such as copper-lead alloy, are more readily obtained in a well-dispersed state by alloy deposition than by thermal means. Alloy plating makes possible the co-deposition of metals or elements, such as tungsten, molybdenum, germanium, and phosphorus, which cannot be deposited from aqueous solution by themselves.

Furthermore, electrodeposited alloys are very often known for their non-equilibrium structure and special properties as compared with normal metallurgical alloys¹. Two common examples of deviations from equilibrium are the formation of supersaturated solid solutions and phases which normally are produced only at elevated temperatures. It is also possible for alloy electrodeposits to exist in metastable phases which do not appear at all on the usual equilibrium phase diagrams.

Developments in this field is, therefore, going on and new alloy coatings are being developed to meet stringent tribological requirements, improved corrosion resistance, heat resistance, surface hardness and so on. Among iron-based alloys, reports on amorphous Fe-W film providing excellent resistance to corrosion², Fe-Cr-Ni alloy coating of 18-8 stainless steel type³, Fe-Ni-W alloy film⁴, Fe-Ni-P⁵ alloy films etc. appeared in the literature recently. The possibility of production of martensitic iron-carbon alloy at room temperature has generated interest very recently. It has been found that Fe-C alloy with quite high hardness (812 HV) and high carbon content (1.2%) could be produced by electrodeposition^{6,7}. This development has great commercial implications as Fe-C coating can replace conventional iron and chromium plating in certain applications. Electrodeposited Fe-C alloy also has the potential of replacing carburising in some cases. Electrodeposition at room temperature offers definite advantages over the conventional high temperature heat treatment used to produce a martensitic structure. These advantages include avoidance of distortion, low energy consumption, low cost etc.

Recently Haseeb and Huq⁸ studied the effect of deposition current density and bath composition on the incorporation of carbon into iron deposits and their hardness. Fe-C deposits with hardness as high as 780 HV and carbon content above 1% were obtained in that study. The coating, however, seem to be rather brittle and not suitable for engineering applications. In order to make it suitable for engineering use its ductility needs to be improved.

The present work is intended to improve the ductility of the Fe-C alloy coatings and this was attempted through the use of additives in the plating bath and through post-deposition heat treatment. In addition, other mechanical properties of the coating viz. hardness, wear resistance were also investigated. Characterization of the coating was done by chemical analysis, X-ray diffraction, optical microscopy and differential scanning calorimetry. Consequently, the effect of process variables like bath composition, current density on the electrochemically deposited alloys was investigated.

2. LITERATURE REVIEW

2.1 Electrodeposition of alloys

2.1.1 General conditions for electrodeposition of alloys

Superficially, the procedure for depositing an alloy differs in no important respect from that for depositing a single metal — a current is passed from electrodes through a solution and a metal deposits upon the cathode. However, the problem of finding conditions for depositing a given alloy in the form of a sound, strong, homogeneous coating is not as easily solved as for a single metal. The simultaneous deposition of two or more metals without regard to the physical nature of the deposit is a relatively simple matter, for it is necessary only to electrolyze a bath of the mixed metallic salts at a sufficiently high current density. Unfortunately, the deposits so obtained are usually loose, spongy, nonadherent masses, contaminated with basic inclusions. Thus, the use of a high current density per se is not a means of solving the problem of alloy deposition.

A preliminary and rather obvious requirement for codeposition of two or more metals from aqueous solution is that at least one of the metals be individually capable of being deposited from aqueous solution.

The most important practical consideration involved in the codeposition of two metals is that their deposition potentials be fairly close together. The importance of this consideration follows from the well known fact that the more noble metal deposits preferentially, frequently to the complete exclusion of the less noble metal. To simultaneously codeposit the two metals, conditions must be such that the more negative (less noble) potential of the less noble metal can be attained without employing an excessive current density. Hence, the need for having the potentials of the two metals close together.

2.1.2 Principles of alloy deposition

The six principles of alloy deposition are:

1. If an alloy plating bath, which is in continuous operation, is replenished with two metals in a constant ratio, M/N (for example, by adding metallic salts or by the use of soluble anodes), the ratio of the metals in the deposit will approach and ultimately take on the value M/N .
2. An increase in the metal-percentage (or ratio) of a parent metal in an alloy plating bath results in an increase in its percentage (or ratio) in the deposit.
3. In alloy deposition, the ratio of the concentration of the more readily depositable metal to the other is smaller at the cathode-solution interface than in the body of the bath.
4. In the deposition of alloys from the normal alloy plating systems, the most fundamental mechanism is the tendency of the concentrations of the metal ions at the cathode-solution interface to approach mutual equilibrium with respect to the two parent metals.

Both principles 3 and 4 lead to the relation

$$C_m/C_n < C_m^0/C_n^0$$

where C_m and C_n are, respectively, the concentrations of the more readily and the less readily depositable metal at the cathode-solution interface, and C_m^0 and C_n^0 are the concentrations of the metals in the body of the bath.

5. A variation in a plating condition that brings closer together the potentials for the deposition of the parent metals separately — that is decreases the interval of potential between them — increases the percentage of the less noble metal in the electrodeposited alloy, and vice versa.
6. In depositing alloys in which the content of the less noble metal increases with current density, the operating conditions for obtaining the more constant composition of deposit are: (i) constant potential if the

uncontrollable variables affect the potentials of the more noble metal and (ii) constant current density if the uncontrollable variables affect the potentials of the less noble metal. Conditions (i) and (ii) are interchanged if the content of the less noble metal decreases with current density.

2.1.3 Types of alloy plating systems

The five types of alloy plating systems are given below —

I. Regular codeposition

Regular codeposition is characterized by the deposition being under diffusion control. The effects of plating variables on the composition of the deposit are determined by changes in the concentrations of metal ions in the cathode diffusion layer and are predictable from simple diffusion theory. The percentage of the more noble metal in the deposit is increased by those agencies that increase the metal ion content of the cathode diffusion layer: increase in total metal content of bath, decrease of current density, elevation of bath temperature, and increased agitation of bath. Regular codeposition is most likely to occur in baths containing simple metal ions, but may occur in baths containing complex ions. It is most likely to occur in baths in which the static potentials of the metals are far apart and with metals that do not form solid solutions.

II. Irregular codeposition

Irregular codeposition is characterized by being controlled by the idiosyncracies of the potentials of the metals against the solution to a greater extent than by diffusion phenomena. The effects of some of the plating variables on the composition of the deposit are in accord with simple diffusion theory and the effects of others are contrary to diffusion theory. Also, the effects of plating variables on the composition of the deposit are much smaller than with the regular alloy plating systems. Irregular codeposition is most likely to occur with solutions of complex ions, particularly with systems in which the static potentials of the parent metals are markedly affected by the concentrations of

the complexing agent, for example, the potential of copper or zinc in a cyanide solution. Irregular codeposition, also, is most likely to occur in systems in which the static potentials of the parent metals are close together and with metals which form solid solutions. It is the least well characterized of the five types and is to some extent a catch-all for alloy plating systems that do not fit one of the other four types.

III. Equilibrium codeposition

Equilibrium codeposition is characterized by deposition from a solution which is in chemical equilibrium with both of the parent metals. The equilibrium alloy plating system is unique in that the ratio of metals in the deposit (plated at a low current density) is the same as their ratio in the bath. Only a few alloy plating systems of this type have been investigated. These are the copper-bismuth and lead-tin alloys deposited from an acid bath and perhaps copper-nickel alloys deposited from a thiosulfate bath. Alloy plating systems which have the same metallic (and other) constituents as the equilibrium system, but not in the equilibrium ratio, behave as their regular or irregular alloy plating systems.

IV. Anomalous codeposition

Anomalous codeposition is characterized by the anomaly that the less noble metal deposits preferentially. With a given plating bath, anomalous codeposition occurs only under certain conditions of concentration and operating variables. Otherwise the codeposition falls under one of the three other types. Anomalous codeposition can occur in baths containing either simple or complex ions of the metals. Anomalous codeposition is rather rare. It is most frequently associated with the electrodeposition of alloys containing one or more of the three metals of the iron group: iron, cobalt, or nickel.

V. Induced codeposition

Induced codeposition is characterized by the deposition of alloys containing metals, such as molybdenum, tungsten, or germanium, which cannot be deposited alone. However, these metals readily codeposit with the iron group metals. Metals which stimulate deposition are called inducing metals, and the metals which do not deposit by themselves are called reluctant metals. The effect of the plating variables on the composition of the alloys of induced

codeposition are more vagarious and unpredictable than the effects on the composition of alloys of any of the other types of codeposition.

2.1.4 Effect of plating variables on the composition of the alloy deposit

2.1.4.1 Introduction

The composition of an electrodeposited alloy is a function of a large number of variables, the main ones of which are as follows:

A. Variables of bath composition

1. Concentrations of depositable metals
 - a. Ratio of the concentrations of the depositable metals to each other
 - b. Total concentration of the depositable metals
2. Concentration of complexing agents
3. pH of plating bath
4. Presence of addition agents
5. Presence of indifferent electrolytes or conducting salts

B. Variables of bath operation

1. Current density
2. Temperature
3. Agitation of bath or movement of cathode

C. Miscellaneous variables

1. Cathode current efficiency
2. Shape of cathode (composition dispersion)
3. Basis metal
4. Thickness of deposit
5. Type of current

2.1.4.2 Concentration of depositable metals in the bath

Probably the most important variables governing the composition of electrodeposited alloys are the concentrations of the two or more parent metals in the bath. In general, the ratio of metals in an electrodeposited alloy differ considerably from their ratio in the bath. Only under special conditions are the ratios of the metals the same in both the bath and the alloy.

The concentrations of the parent metals in the bath can be varied by three methods:

(a) Variation of metal ratio: The total metal content of the bath is kept constant while the ratio of one metal to the other is varied. This method is the most important because the composition of the alloy is more responsive to the metal ratio of the bath than to any other variable.

(b) Variation of total metal content: The ratio of the two parent metals in the bath is kept constant while the total metal concentration is varied.

(c) Variation of concentration of a single metal: The concentration of one parent metal is kept constant in the bath while increments of the other parent metal are added.

The relation between the composition of the electrodeposited alloy and the ratio of the parent metals in the bath is the most important relation in alloy plating system. One feature of Figs 2.1 and 2.2 is that they contain an auxiliary line, AB, which will be referred to as the "composition-reference line". It is aid in visualizing the relation between the percentage composition of the alloy and the metal-percentage of the bath. Points falling upon the composition reference line would represent alloys having the same percentage composition as the metal-percentage of the bath. A composition curve that raises above the composition-reference line indicates that the metal in question is preferentially deposited, because its percentage in the deposit is larger than its metal percentage in the bath. In normal codeposition, the more noble metal deposits preferentially, hence the curve for the percentage of the more noble metal in a deposit always lies above the composition reference line. Similarly, the curve representing the percentage of the less noble metal plotted against its metal-percentage in the

bath lies below the composition reference line.

Examples of normal codeposition are illustrated in Fig. 2.1. Curves 1-3, respectively, represent regular, irregular, and equilibrium codeposition. Curves 1 and 2 represent the plot of the percentage of the more noble metal, copper, in the alloy against its metal-percentage in the bath, and consequently these curves lie above the composition-reference line AB.

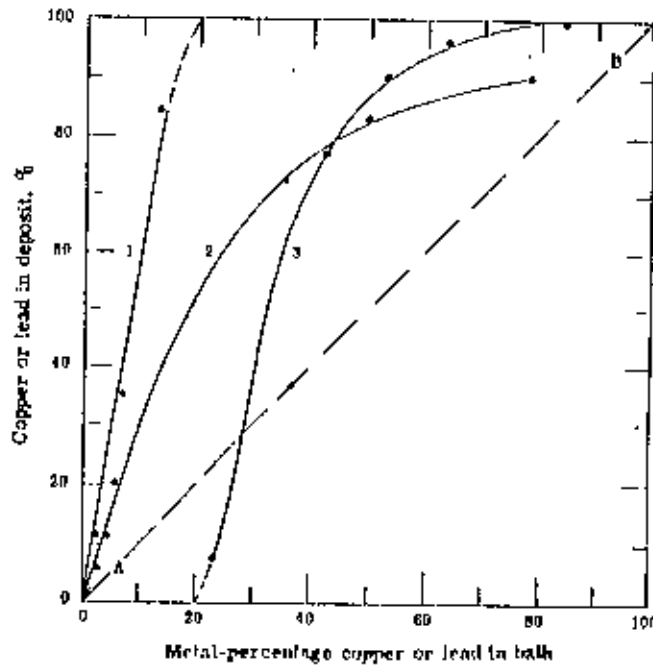


Fig. 2.1 Typical curves illustrating the relation between the composition of electro-deposited alloys and the composition of the bath in normal co-deposition.

Curve 1: Bismuth-copper alloys deposited from perchlorate bath⁹

Curve 2: Copper-zinc alloys deposited from cyanide bath^{10,11}

Curve 3: Lead-tin alloys deposited from a fluoborate bath^{1,2}

Fig 2.2 illustrates the relation between the composition of the deposit and the composition of the bath in anomalous codeposition. Three different alloys, iron-zinc (curve 1), nickel-zinc (curve 3) and cobalt-nickel (curve 2), all deposited from simple chloride or sulphate baths are used as examples. The outstanding feature of this figure is that the composition curves for the more noble metals, nickel and iron, lie below composition-reference line, AB, in contrast to curves 1 and 2 of Fig 2.1. This means that although iron and nickel are the more noble metals, they are not preferentially deposited. The data for curve 3, representing deposition of nickel-zinc alloys, comes from the work of Schoch and Hirsch¹³ which was done in 1907 and is one of the earliest studies of the principles of alloy deposition. Although the total metal content of their baths varied widely, this does not vitiate the relation between the metal ratio of the bath and the deposit.

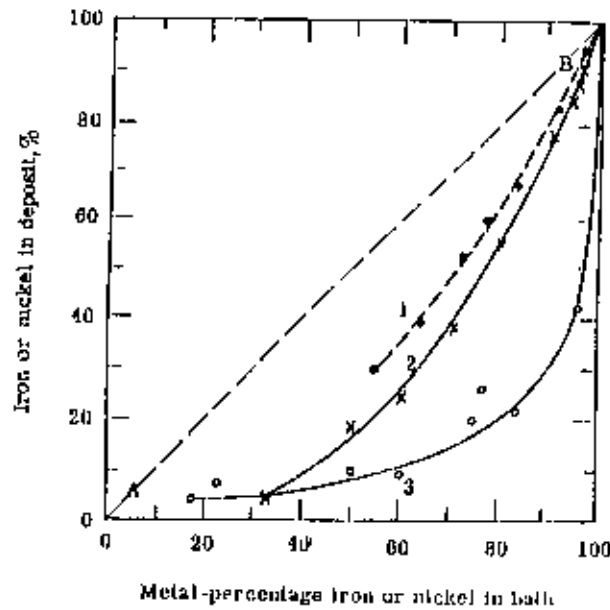


Fig. 2.2 Relation between the composition of the deposit and the composition of the bath in anomalous co-deposition.

Curve 1: Iron-zinc alloys deposited from sulphate bath¹⁴

Curve 2: Nickel-cobalt alloys deposited from chloride bath¹⁵

Curve 3: Nickel-zinc alloys deposited from sulphate bath¹³

The behavior of metals in anomalous codeposition is not as consistent and clear-cut as would appear from the curves shown. Under some conditions of current density and temperature, the metals may codeposit in a normal fashion and under other conditions in an anomalous fashion.

Variation of the total metal content of a bath, at a fixed metal ratio, appreciably affects the composition of alloys in regular codeposition but has either slight effect or no uniform trend in irregular, anomalous and induced codeposition.

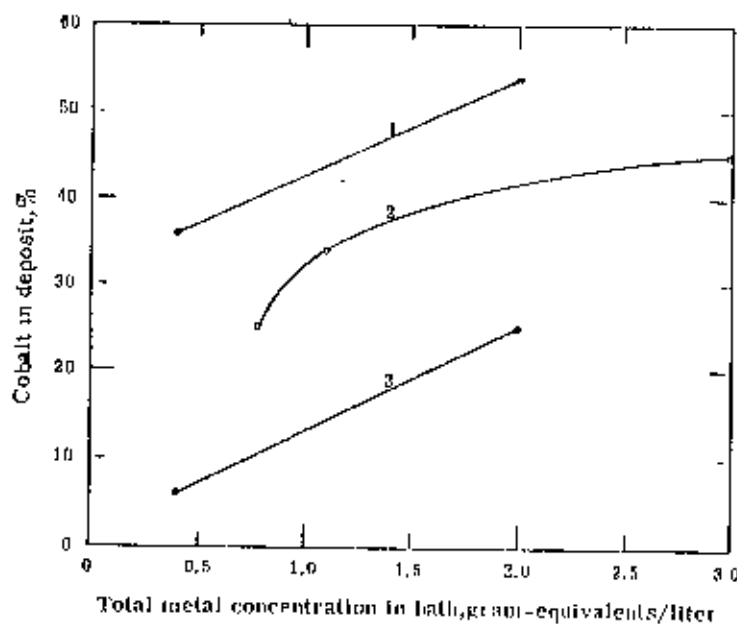


Fig. 2.3 Relation between the composition of the deposit and the total metal content of the bath in anomalous co-deposition.

Curve 1 and 3: From the data of Glasstone and Speakman¹⁶

Curve 2 : From the data of Fink and Lab¹⁷

The effect of total metal content of the bath on the composition of the deposit in anomalous codeposition is illustrated in Fig. 2.3. With data on the deposition of cobalt-nickel alloys taken from the work of Glasstone and Speakman¹⁶ and Fink and Lah¹⁷. The alloys were deposited from simple sulphate baths. Cobalt deposited preferentially although it is less noble than nickel. The curves show that for a sevenfold increase in total metal content of the bath, the cobalt content of the deposit increased only slightly. Comparison of these curves with the much steeper curve 2 of Fig. 2.2 shows the much greater effect of varying the metal ratio of the bath.

2.1.4.3 Concentration of complexing agents in the bath

Since complexes are so potent in bringing about codeposition of metals, it is to be expected that the composition of an electrodeposited alloy would be affected by the concentration of the complexing agent. Indeed, next to the metal ratio of the bath, the concentration of the complexing agent has the greatest influence on the composition of the deposit. The general effect of increasing the concentration of a complexing agent is to make the deposition potentials of a metal more negative (less noble), so that the metal becomes less readily deposited. In an alloy plating bath, if an increase in concentration of the complexing agent shifts the deposition potential of one metal more than that of the other, a diminution in the percentage of the former metal in the deposit results.

Only in the mixed type of plating bath is the composition of the deposit markedly affected by the concentration of the free complexing agents. The reason for this is that in a mixed bath, the deposition of each parent metal is responsive only to the concentration of its particular complexing agent. On the other hand, in a "single complex" bath an increase in the concentration of the complexing agent shifts the potentials of both parent metals to more negative (less noble) values, and, *a priori*, one cannot tell whether the effect on the potential of one metal will be relatively greater or smaller than that on the other. Consequently, the effect of concentration of the complexing agent in single complex baths is neither readily predictable nor very large in magnitude.

2.1.4.4 pH

The effects of pH on the composition of an electrodeposited alloy are specific and usually unpredictable. In some baths, the pH has a large effect and in others a small effect on the composition of the deposit. The determining factor is the chemical nature of the metallic compounds, because the pH does not exert its effect per se but by altering the state of chemical combination of the metals in solution. Simple metallic ions are only slightly sensitive to variations in the pH of the solution; this is indicated by a slight variation in the thermodynamic activity of the ion. On the other hand, the composition and stability of many complexes — in both alkaline and acid solution — are a function of the pH. For example, complexes, such as stannate, zincate, cyanides, and amines, which are stable in alkaline solution, decompose when acidified. As a general rule, variations of pH should have little effect on the composition of alloys deposited from baths containing the metals as simple ions and should have a large effect on the composition of alloys deposited from baths in which the parent metals were present as complexes with large instability constants.

Glasstone and Speakman^{16,18} determined the most noble potentials at which the iron-group metals and their mutual alloys deposited from solutions of various pH. They did this by gradual increasing the current density and noting the potential at which codeposition was initiated. As might be expected, the more acid the solution, the higher was the current density required to initiate metal deposition. However, rather unexpected was the finding that the potentials at which deposition was initiated was about the same in the solutions of various acidity, since the potential of initial deposition was independent of the pH of the bath, one might surmise that the composition of the electrodeposited alloys might also be little influenced by variations in pH.

Fig. 2.4 shows data from three curves. Curve 1 represents data from Young and Strutk¹⁵ for the deposition of Co-Ni alloys from a simple salt bath. Curve 2 represents data from Glasstone and Symes¹⁹ for the deposition of Fe-Ni alloys from a sulphate bath. Curve 3 is the data of Raub²⁰ for deposition of Fe-Ni alloys from a bath containing citric acid. The three curves all represent anomalous codeposition since Ni, the more noble metal, occurs in the deposit in a smaller percentage than its metal-percentage in the bath, which was 90% or more.

The curves show that the composition of the deposit is little affected by pH up to 5. This is in accord with the surmise based on the work of Glasstone and Speakman, mentioned previously, and in accord with the general proposition that pH has little effect on deposition from baths containing simple metallic ions. The large increase in the Ni-content of the deposit shown by curve 3 is doubtlessly caused by the complexing of the iron with citrate ion, when the pH of the bath was increased above 6.

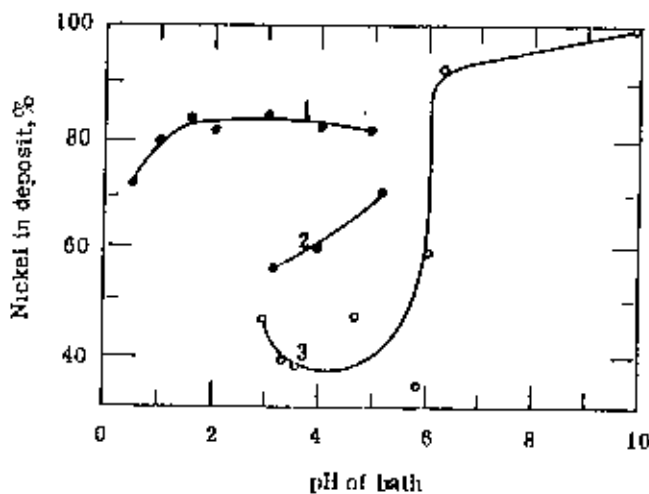


Fig. 2.4 Effect of pH on the composition of deposits in anomalous co-deposition.

Curve 1: Cobalt-nickel alloys from the data of Young and Struyk¹⁵

Curve 2: Iron-nickel alloys from the data of Glasstone and Symes deposited from sulphate bath¹⁹

Curve 3: Iron-nickel alloys from the data of Raub deposited from a bath containing citric acid²⁰

2.1.4.5 Current density

Current density is the most important of the operating variables, and no study of alloy deposition is complete without detailed data on the variation of alloy composition with current density. The effect of current density is less consistent or predictable than that of the other operating variables, with respect to both the magnitude and the sense of the variation in composition of the electrodeposited alloy.

The mechanism may be examined from two view points, diffusion control and the cathode potential. With regard to the latter, an increase of current density causes the cathode potential to become more negative (less noble) and hence, the plating conditions approach more closely to those represented by the current density-potential curve of the less noble metal. *A priori*, this condition should increase the proportion of the less noble metal in the deposit. According to simple diffusion theory, the rate of diffusion of a metal has an upper limit which is determined by the rate at which its ion can move through the cathode diffusion layer. At a given current density, the rate of deposition of the more noble metal is relatively much closer to its limiting value than that of the less noble metal. An increase of current density, therefore, must be borne mainly by an increase in the rate of deposition of the less noble metal.

In the regular type of codeposition, the content of the less noble metal in the deposit increases with current density. However, in other types of codeposition the opposite relation frequently occurs and in some instances the content of one of the metals goes through a maximum or minimum as the current density is varied. These departures from the expected qualitative relations are difficult to explain. In some instances they may not be bona fide effects of current density, but may be the result of inadequate control of the plating conditions during the experiment.

The magnitude of the changes in alloy composition resulting from variation of current density are rather large for the regular type of codeposition and small for the other types of plating systems. However, no general rule can be given since the effects depend on specific properties of each alloy plating system.

In Fig. 2.5, curve 1 represents the deposition of Fe-Zn alloys from an acid sulphate bath at 90°C. The data are from the work of Von Escher and others²¹. The point P indicates the metal percentage Zn in the bath, which is 11.5%. The curve consists of three branches. In the low current density region, from a to b, the codeposition appears to be of normal type, that is, the deposit contains a smaller content of the less noble metal, Zn, than corresponds to the metal-percentage Zn, P in the bath and with increasing current density increases in Zn content and above 2.5 Amp/dm² contains much more Zn than corresponds to the metal-percentage Zn in the bath.

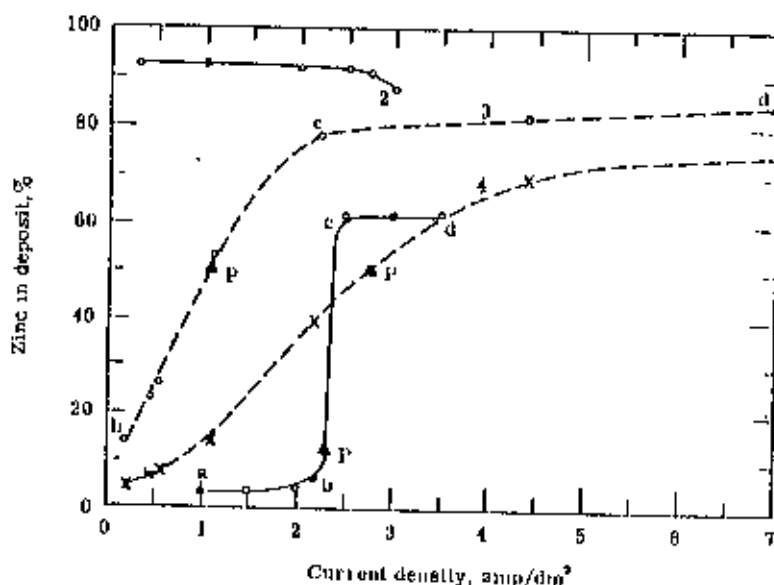


Fig. 2.5 Relation between alloy composition and current density in anomalous co-deposition.

Curve 1 and 2: Iron-zinc alloys deposited from acid sulphate bath²¹

Curve 3 and 4: Nickel-zinc alloys deposited from acid chloride bath²².

The transition of the Zn content of the deposit from a value well below, to a value well above, the metal-percentage Zn of the bath occurs over a rather small range of current density (branch bc). The current density at the point P is referred to as 'transition current density'.

The third branch of curve 1, from c to d, exhibits little change in alloy composition with current density. Since Zn is depositing preferentially, the cathode film must be relatively more depleted in Zn than in Fe. Consequently, the deposition should be under diffusion control and the Zn content of the deposit should tend downwards at still higher current density. This fourth type of relation, illustrated by branch de, is not shown by curve 1 but is shown by curve 2. Curves 3 and 4 for the deposition of Ni-Zn alloys from an acid chloride bath²² show only two branches. The low current density region from a to b missing.

2.1.4.6 Temperature

The effect of temperature on the composition of electrodeposited alloys may be the net result of changes in several characteristics of the plating system, such as the following:

1) Equilibrium potential: The equilibrium or the static potentials of the metals may change. This is probably not an important factor since the equilibrium potentials of metals do not change greatly with temperature, and furthermore electrodeposition is far removed from equilibrium conditions.

2) Polarization: The deposition potentials of metals usually become more noble with increase in temperature, because polarization is decreased. Whether the deposition of the more noble or less noble metal is favoured depends on which deposition undergoes the largest decrease in polarization. These effects are specific and therefore, the effects of temperature, via polarization, cannot be predicted without actual measurements on the deposition potentials of each of the metals.

3) Concentration: An increase in temperature increases the concentration of metal in the cathode diffusion layer, because the rates of diffusion and of convection increase with temperature. This is the most important mechanism by which temperature affects the composition of electrodeposited alloys. According to principle 2, an increase in metal concentration at the solution-cathode interface favors increased deposition of that metal which already was depositing preferentially. Since regular alloy plating systems, the more noble metal always deposits preferentially, the effect of temperature is always to increase the content of the more noble metal in the deposit.

4) Cathode current efficiency: Temperature may affect the composition of an electrodeposited alloy indirectly through its effect on the cathode current efficiency of deposition of the metals, particularly those deposited from complex ions. For example, an increase in temperature increases the cathode current efficiency of deposition of tin from a stannate bath, and of copper from a cyanide bath. In electrodeposition tin or copper with other metals whose efficiencies of deposition are unaffected by temperature, the tin or copper content of the deposit will increase regardless of whether tin or copper happen to be the more noble or the less noble of the pair.

Of the above four factors, (3) and (4) are the most important.

2.1.4.7 Bath agitation

Agitation of an alloy plating bath or rotation of the cathode can directly affect the composition of the alloy by reducing the thickness of the cathode diffusion layer. This is a purely mechanical action which does not change the electrochemical properties of the solution or the mechanism of the plating process. Being of this nature, agitation has a more consistent influence on the composition of the deposit than either temperature or current density.

The effect of agitation on the composition of the deposit is due to the concentration changes which it produces at the cathode-solution interface. During alloy deposition the cathode diffusion layer is depleted in metal ions and, furthermore, the ratio of the concentrations of the metals in the layer differs from that in the body of the bath. Agitation of the bath or rotation of the

cathode, by decreasing the thickness of the cathode diffusion layer not only results in an increase in the concentration of metal ion in the cathode diffusion layer, but also causes the metal ratio of the diffusion layer to approach more closely to that of the solution in the body of the bath. According to principle 2, this favors an increase of that metal which is already depositing preferentially. The effect of agitation, thus, is similar to that of increasing the concentration or the temperature of a bath, except that temperature is a more complicated variable than agitation, inasmuch as it is associated also with other phenomena, such as polarization.

2.1.4.8 Addition agents

An addition agent is a substance which, when present in a plating bath in a small concentration relative to that of the metal, produces desirable effects on the appearance of the deposit; for example, it reduces grain size and, thus, improves the smoothness and brightness of the deposit and decreases the tendency of the deposit to tree. Because many of the addition agents first used were organic substances of high molecular weight, such as gelatin, proteins, and organic extracts, addition agents were considered to be colloids. However, the large number of addition agents which have been subsequently utilized do not have any common chemical characteristic. They may be either organic or inorganic in nature and are generally not colloids.

Addition agents, in the small concentrations that are normally used, do not have an appreciable effect on the properties of the plating solution. They do not significantly affect the viscosity, conductivity, pH, metal ion concentration, or the static electrode potential. Therefore, their effectiveness is not related to any of these factors. In contrast to their lack of effect on static electrode potentials, addition agents usually have a considerable effect on dynamic electrode potentials. In most instances, addition agents increase cathode polarization but do not have much effect on anode polarization. However, addition agents can lower the polarization of metal deposition, particularly if the deposition normally occurs with a high polarization. Examples of this less common phenomenon are the presence of carbon disulfide in a silver cyanide plating bath and the presence of sodium thiosulfate in a copper cyanide plating solution.

The presence of addition agents in a plating bath brought the deposition potentials of metals closer together and thus enabled codeposition to take place. Since addition agents can bring about codeposition, it is to be expected that their concentration should have a considerable effect on the composition of the electrodeposited alloy, similar to the effects of complexing agents.

In Fig. 2.6 are given two examples of the effect of addition agents on the composition of an alloy deposit. The data for the zinc-cadmium curve was taken from the work of Fink and Young²³, which was carried out with a simple sulfate

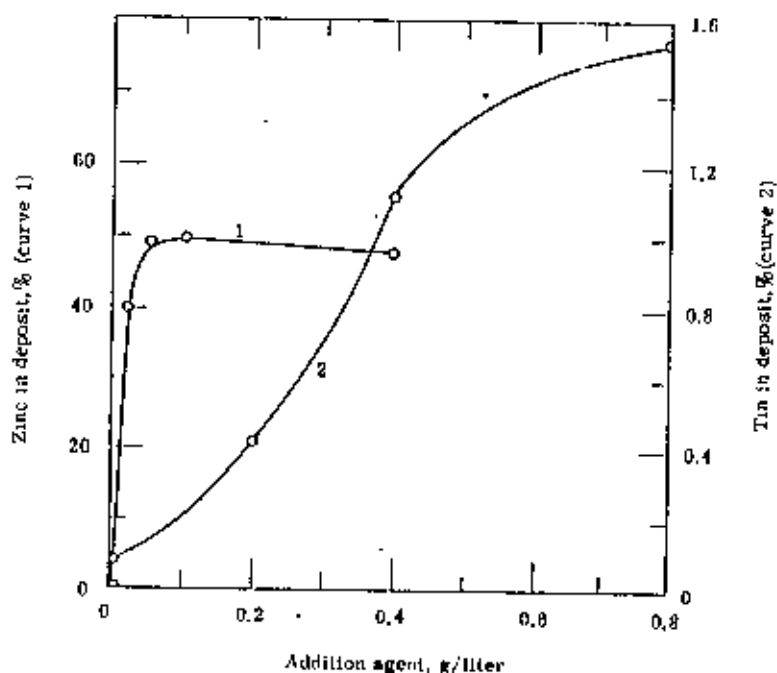


Fig. 2.6 Effect of addition agents on the composition of electrodeposited alloys

Curve 1: Zinc-cadmium alloy deposited from a sulphate bath containing aloin as additive²³

Curve 2: Lead-tin alloy deposited from a fluoborate bath containing glue as additive²⁴

bath. The data for the tin-lead alloy was taken from the work of Du Rose²⁴. The ordinates giving the per cent of tin are on the right of the figure. The deposits were plated from fluoborate baths in which the metal ions are of the simple type. The curve show that small concentrations of addition agents produced large changes in the composition of the deposit. The composition of the alloy changed rapidly with the initial additions of the agent and then tended toward a limiting value which was not appreciably affected by further increases in the concentration of the addition agent.

The relation between the composition of the deposit and the concentration of the addition agent differs from that for complexing agents in the following ways: (1) The concentration of an addition agent required to produce an appreciable effect is much smaller than that of a complexing agent. (2) With the addition agent the composition of the deposit rapidly approaches a limiting value.

Addition agents usually are most effective in baths containing the metals as simple ions, as in the two examples just given. Also, it will be noted that in both examples it was the less noble metal whose content in the deposit was increased by the addition agent. This is generally the case but exceptions are known.

The effect of the addition agents is specific. Only certain agents affect the composition of the deposit, and the magnitude of the shift in composition produced by different agents varies considerably. For example, if resorcinol were added to the tin-lead bath, the tin content of the deposit would rise above 6% as compared to about 1.6% with glne alone.

2.2 Structure of electrodeposited alloys

The microstructure of electrodeposited alloys is in many respects similar to that of the individually deposited metals in that the grain size is similar than that of thermal alloys, and laminations parallel to the basis metal occur frequently. The grain size of an electrodeposited alloy is even smaller than that of its parent metals, individually deposited; only seldom can grains be seen under the microscope, and even less seldom can individual phases be distinguished and identified. In contrast, in thermally prepared two-phase alloys usually one phase

is held in a matrix of the other in the form of dendrites or equiaxed crystals, and the two phases are usually visible under the microscope. This comparison shows that the constituents of a polyphase electrodeposited alloys are much more thoroughly intermingled than those of a thermal alloy, that is, the electrodeposited alloy usually has an ultrafine structure.

The examination of the cross-section of deposits is of more interest than that of the surface. A cursory examination of the photographs of cross-sections shows that the microstructure of electrodeposited alloys does not resemble that of thermal alloys. The latter usually exhibit a fairly definite pattern of grains or crystallines, usually equiaxed, whereas the former usually exhibit a fibrous, columnar structure, or a laminar structure, or both.

The phases which are present in electrodeposited alloys very seldom can be recognized or even distinguished microscopically. For this reason the few cases in which this has been done are worthy of mention. Lustman²⁵ observed alpha and beta phases in electrodeposited nickel-zinc alloys. They were distinguishable by the customary etching procedures, the former phase appearing yellowish-white and the latter dark brown. In the electrodeposited silver-cadmium alloy, containing 10% of silver, Faust and co-workers²⁶ observed two phases, one of which resembled the light-colored epsilon and the other, the dark-colored eta phase of the thermal alloy.

When metals are codeposited under unsatisfactory conditions that yield unsound deposits of poor physical characteristics, the deposits are often sufficiently heterogeneous for the individual metals to be observed in the deposit. For example, in their study of the deposition of silver-bismuth alloys from a cyanide bath, Raub and Eugel²⁷ observed that alloys containing up to 3% of bismuth appeared homogeneous under the microscope, but alloys higher in bismuth consisted of two phases and were heterogeneous, nonuniform, and brittle. The point to be emphasized here is that heterogeneity of an alloy deposit is to be construed as evidence of unsatisfactory conditions of codeposition rather than as a characteristic of electrodeposited alloys.

Nakamura²⁸ made the earliest study of the phases present in electrodeposited alloys. He showed that electrodeposited brass, containing 82% of copper, had the same lattice parameter as cast alpha-brass of the same composition. His work was followed by that of Roux and Cournot^{29,30} in 1929 on electrodeposited

copper-zinc, cadmium-silver, cadmium-tin, and cadmium-nickel alloys. By comparing the diffraction patterns of the electrodeposited alloys with those of the individual metals and by measuring the lattice parameters, they demonstrated that these alloys were not gross mixtures of the metals, but consisted of phases similar to those in the thermally prepared alloys.

The differences which may exist between the structures of electrodeposited and thermally prepared alloys are of various kinds and require detailed discussion. Basically, the differences in structure can be considered as due to differences in the range of composition or temperature over which the phases exist:

- 1) Phases in electrodeposited alloy may exist over a larger range of composition than in the thermally prepared alloy. These phases usually are solid solutions containing a fair proportion of each of the parent metals. A more unusual widening of the range occurs with some metals like copper and lead which have no appreciable mutual solid solubility. On electrodeposition they may form a supersaturated solid solution.
- 2) The range of existence of a phase may be smaller in the electrodeposited alloy. In the extreme case, a phase that occurs in the thermal alloy may be missing from the electrodeposited alloy. For example, in electrodeposited speculum metal the epsilon phase is absent, its place being taken by the expanded range of composition of the two neighbouring phases³¹. Gold and copper furnish another example. These metals codeposit as virtually the individual metals³², whereas the thermally prepared alloys consist of an unbroken series of solid solutions.
- 3) The phases of electrodeposited and thermally prepared alloys may differ with respect to the temperature at which they are produced. For example, in cast speculum metal, the gamma phase is not formed below 520°C, but it occurs in speculum metal³⁰ electrodeposited at room temperature. The phase is probably metastable at room temperature.
- 4) The lattice parameters of codeposited metals or of their phases may be slightly different from those of the cast alloy. In many instances this is difficult to determine with certainty because of line broadening.

The differences in the phases of electrodeposited and thermally prepared alloys of the same percentage composition may be summarized on the basis of the discussion under (1) and (2). An electrodeposited alloy may have either more or less phases than indicated by the constitutional diagram. For example, it may consist of only one phase when two should be present or it may consist of two phases when only one should be present.

2.3 Effect of heat treatment on microstructure

The effect of heat treatment on the structure of electrodeposited alloys cannot be fully discussed until the subject of X-ray examination has been taken up. At this point only the obvious effects of heat treatment as revealed by the microstructure of cross-sections are considered. The effects of heat treatment on alloy deposits have been particularly studied by Brenner and co-workers³³ in connection with tungsten alloys and phosphorus alloys³⁴, by Ranb and coworkers³⁵ in connection with copper-lead, silver-lead, and silver-bismuth alloys; and by Aotani^{36,37} in his studies of the codeposition of iron-group metals.

The change in the structure of an electrodeposited alloy depends on the temperature of heat treatment. For example, at a temperature of 500°C the laminar structure of some alloys containing an iron-group metal becomes more diffuse and may disappear. The fibrous structure, if present, usually persists at slightly higher temperatures than the laminated structure. At the more elevated temperatures of 800°C or 1000°C, these characteristic structures disappear and recrystallization takes place. The grains are usually much smaller than those of the thermal alloy or of the parent metals when similarly annealed. However, the phases present in the recrystallized electrodeposited alloys are the same as those in the corresponding thermal alloy.

Suitable heat treatment of an alloy of any kind causes its structure to approach an equilibrium condition. Electrodeposited alloys which consist of supersaturated solid solutions, for example, copper-lead or silver-lead alloys, break down into the component metals. Electrodeposited alloys, consisted of individual metals, which normally form solid solutions, such as copper-gold or

silver-cadmium alloys, are also metastable. On heat treatment the individual metals of the alloy mutually dissolve to form the equilibrium solid solutions. These changes in microstructure and internal structure are accompanied by changes in physical and mechanical properties.

The temperatures and the periods of heating required to bring the structure of electrodeposited, supersaturated alloys to equilibrium are lower than those required for nonequilibrium thermal alloys, for example, those which have been prepared by rapid cooling. The rate at which the supersaturated electrodeposited alloys approaches equilibrium does not seem to vary appreciably with the degree of supersaturation of the alloy, in which respect they differ from thermal alloys. Electrodeposited alloys behave as if at low degrees of supersaturation they already possessed the maximum instability.

2.4 Structure of electrodeposited alloys as revealed by X-ray

By far the most important means of investigation the structure of electrodeposited alloys is by X-rays. The initial reason for the considerable interest was the desire to establish whether codeposited metals were really alloys or merely gross admixtures of two metals. The X-ray studies clearly demonstrated that electrodeposited alloys are true alloys, having structures similar to those of the thermally prepared alloys.

X-rays are a powerful tool for elucidating structure, but it must be recognized that they have certain limitations. X-rays are not a sensitive means of detecting the components in a mixture. Usually a component must be present in a mixture to the extent of at least 5% before its diffraction pattern becomes distinct enough to be recognized against the patterns of the other substances. Thus, the recognition of small contents of one phase in the presence of a large quantity of another may not be possible, and the establishment of the limits of the composition of a phase by X-rays may be only approximate and must be supplemented by other types of observations, such as microscopic examination and measurement of electrical conductivity.

These limitations to the use of X-rays for studies of structure apply to thermal alloys as well as electrodeposited alloys. However, the X-ray examination of electrodeposited alloys is hampered by some additional difficulties which do not occur with thermal alloys. The diffraction patterns of the electrodeposited alloys are usually diffuse, which makes the accurate measurement of the lattice parameters difficult. The diffuseness of the lines in the diffraction pattern can have several origins:

- 1) inhomogeneities in the composition of the alloy
- 2) lattice distortion, due to internal stresses, similar to those induced by cold working
- 3) small grain size

Two or more of these factors could be operative at the same time. This subject was first discussed by Dehlinger and Giesen³⁸ in their study of the structure of brass deposits. Since the line broadening did not disappear after the deposits were annealed at 300°C, they considered that it could not be caused by stress, which would have been removed by the heat treatment. They also discounted the possibility that it could be the result of a lack of uniformity in the composition of the deposit by the following line of reasoning. The differences in composition would have to be of the order of several per cent to account for the broadening. They showed that an anneal at 400°C for only 10 minutes sufficed to eliminate the line broadening. In this short period of time diffusion would not have been sufficiently rapid to eliminate the nonuniformity had it been present, and therefore the only mechanism capable of producing the change was grain growth.

The causes of line broadening were also discussed by Montoro^{39,40} in connection with the structure of copper-tin and copper-lead alloys. He considered the possibilities (2) and (3) mentioned previously, and in addition, the possible effects of inclusions of hydrogen and other impurities. Since the line broadening did not occur to any significant extent with the individually deposited metals, which would be exposed to the same influences as the alloy, he came to the conclusion that these factors could not be responsible for the line broadening and believed that the nonuniformity of the specimen was the more likely cause.

There is no doubt that nonuniformity of composition can cause line broadening and also it is quite likely that some of the line broadening observed by Montoro and others may have been due to this source. However, many of the alloys which have been examined by X-rays must have been fairly uniform in composition and, on the other hand, some electrodeposits, such as bright nickel and chromium, yield diffuse diffraction patterns because of their small grain size. Therefore, the best view of the matter is that diffuseness of the diffraction patterns of electrodeposited alloys results mainly from small grain size, and that superimposed upon this may be a diffuseness due to nonuniformity of composition.

The various difficulties involved in X-ray measurements permit only an approximate determination of the range of composition over which a phase exists and the value of the lattice parameter. The latter often shows a considerable scatter when measured on different specimens of the same electrodeposited alloy.

2.5 Mechanical properties of electrodeposited alloys

2.5.1 Introduction

The properties of electrodeposited metals, particularly their mechanical properties, often differ from those of metallurgical metals. In general, electrodeposits tend to be harder, less ductile, and finer grained. As examples, electrodeposited chromium, with its great hardness, is quite different from the soft metal obtained by thermal means. Bright nickel is much harder, has a higher tensile strength, and is much less ductile than cast nickel. The grains of these electrodeposits cannot be seen under the microscope, whereas the crystals of cast metals are observed readily.

The mechanical properties of metallurgical metals may be varied considerably by heat treatment or mechanical working. The properties of electrodeposited metals also may be varied, but this is achieved by altering the conditions of deposition. Indeed, some of the properties of electrodeposited metals, for example, the

hardness, may be made to vary over a much wider range than those of thermally prepared alloys. Obviously, the properties of electrodeposited metals may be varied further by application of heat treatments.

Since electrodeposited alloys, like metallurgical alloys, possess a wider range of properties than the parent metals, they should find more extensive and varied uses than electrodeposits of single metals. However, in contrast to the widespread use of metallurgical alloys, as compared to single metals, for engineering purposes, electrodeposited alloys are much less used than deposits of single metals. This is not because the latter are best suited for the application but because (1) pure metals are easier to deposit than alloys, (2) some of the desired alloys have not yet been successfully deposited, and (3) the properties of the alloys are not adequately known.

2.5.2 Hardness

The hardness of electrodeposits is usually measured by indentation or scratch methods. The use of a pointed diamond indenter, such as a Vicker or Knoop diamond, in conjunction with a light load of 25 to 250 g is the preferred method. The measurements are usually referred to as the microhardness, but they differ from ordinary indentation methods only in that a lighter load is used. The indentations are usually made on a polished cross-section of the deposit, which should be a minimum of about 50 μm (2mils) thick, but measurements can also be made directly on the plated surface parallel to the basis metal.

The hardness of electrodeposited metals is greater than that of cast metals, and in turn the hardness of electrodeposited alloys is greater than that of either of the individually deposited parent metals. The hardness of electrodeposited alloys increases most rapidly with the first small additions of the alloying metal, then at a decreasing rate. The percentage of alloying element, above which the hardness shows little change, depends on the nature of the alloy. For example, the hardness of electrodeposited cobalt-tungsten alloys increased with tungsten content until the latter reached 35-50%. In contrast, the hardness of electrodeposited silver-lead alloys reached its limit when the lead content of the alloy was about 3%, as shown in Fig. 2.7 These data are from Ranb⁴¹. In

general, the reproducibility of the hardness of electrodeposited alloys is not very high, which makes the determination of the trend between alloy composition and hardness rather difficult.

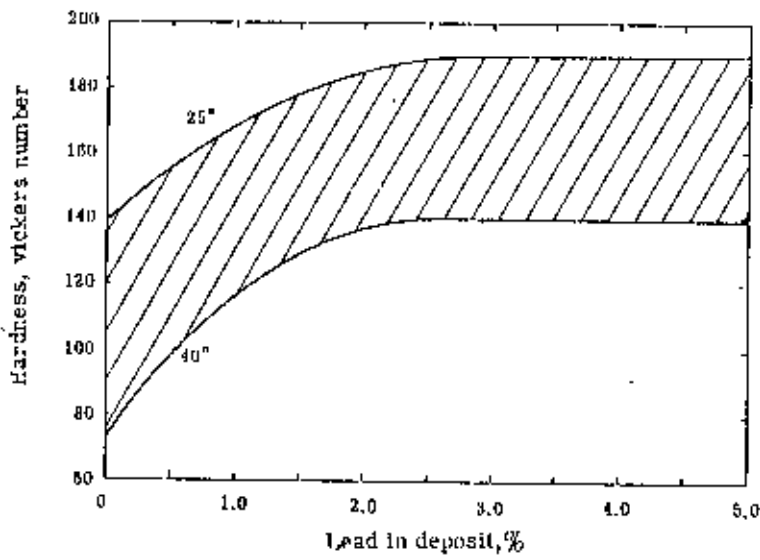


Fig. 2.7 Effect of lead content on the hardness of silver-lead alloys deposited from a cyanide-tartrate type of bath.

2.5.3 Ductility

Ductility is considered to be the ability of a material to undergo the plastic deformation required for the forming operation. In comparison with cast and wrought materials, electrodeposited materials often suffer from a low ductility due to their thin foil geometry⁴². So, many methods such as tensile test, bulge test, stretching test, low frequency fatigue test and bend test have been developed to measure the ductility of thin metallic coatings.

The conventional mechanical testing methods developed for bulk metals are often inadequate for the testing of electrodeposits. Uniaxial tensile tests on samples 25-75 μm thick present a serious problem in preparation and handling⁴³. Cutting or stamping of a specimen from a metallic foil hardly results in a cut-free specimen, and deformation can occur during handling and mounting of thin specimens⁴⁴. A deviation of the sample axis from the true axis of the test machine, or a slight specimen misalignment introduces the nonaxiality of loading, a cause for premature failure⁴³.

The bulge test is a biaxial tensile test. It is done by clamping tightly the foil sample over an opening of a chamber and by applying hydraulic pressure to form a circular bulge. The force is transmitted to the sample by means of the pressure that the liquid (oil or water) exerts on the inside of the sample clamped to the chamber. The pressure is increased until the sample fractures. Then according to the height of the bulge measured with a linear differential transformer and the pressure of the liquid measured with a pressure transducer, the mechanical properties are calculated.

The stretching test is similar to the bulge test, but instead of a liquid, a punch head is utilized to exert the force on the measured foils. In low-frequency fatigue test, specimens are bent on a test mandrel, straightened out, and then bent in the opposite direction. This operation is repeated until fracture is detected. The number of bends to fracture is taken as a measure of the ductility.

Of them, the most widely used approach is some type of bend test in which coated material is deformed in a standardised manner and then the coating is scrutinized for the first evidence of cracking or peeling. There are a lot of bend tests. They can be divided into two groups: specimens bent against a mandrel, or

without any mandrel. The standard recommended practice for bend test for ductility of plated metals consists of bending over a mandrel a narrow piece cut from a metal electroplated article. The elongation measurement is obtained from the smallest diameter mandrel that does not cause the deposit to fracture. The other more frequently utilized methods is the "U" bend test. Foil is bent into a "U" shape and placed between the jaws of a micrometer. The jaws are then slowly closed on the piece until fracture occurs. From the deposit thickness and the size of the opening between the micrometer jaws at fracture, the elongation is then calculated. The reproducibility of bend tests is poor. It is highly questionable whereas the elongation obtained in bending is comparable with that obtained in conventional tensile testing⁴². However bend test is widely used because of its simplicity.

Ductility depends on coating composition, coating thickness, texture, stress ratio, surface roughness, overpotential and other coating characteristics. The uniformity of thickness and width of the specimens surely is a key to get accurate results for the tensile test of thin foils. It has been observed^{45,46,47} that the ductility increases with increasing coating thickness. The ductility decreases with increasing surface roughness, provided other parameters which influence the ductility are kept constant⁴². Except for very ductile deposits, the apparent ductility is an inverse function of the coating thickness⁴⁸. For systematic study of ductility dependence on coating composition, the other parameters must be identical.

According to Marciniak and Kuczynski⁴⁹, the initial topographical irregularity also affect the ductility. The specimens deposited at constant overpotential appear to have larger ductility than those deposited at the same temperature but at constant current density⁴².

2.5.4 Wear resistance

The wear behaviour of materials is a very complicated phenomenon in which various mechanisms and influencing factors are involved. According to Burwell⁵⁰, wear mechanisms may be divided into four broad general classes under the headings of abrasion, adhesion, surface fatigue and tribochemical processes.

The effect of abrasion occurs in contact situations in which direct physical contact between two surfaces is given, where one of the surfaces is considerably harder than the other. The harder surface asperities press into the softer surface with plastic flow of the softer surface occurring around the asperities from the harder surface. When a tangential motion is imposed the harder surface remove the softer material by combined effects of "micro-ploughing", "micro-cutting", and "micro-cracking". Influences of capacity of work-hardening, ductility, homogeneity of strain distribution, crystal anisotropy and mechanical instability have been identified to influence the abrasive wear mechanisms⁵¹ (Fig. 2.8).

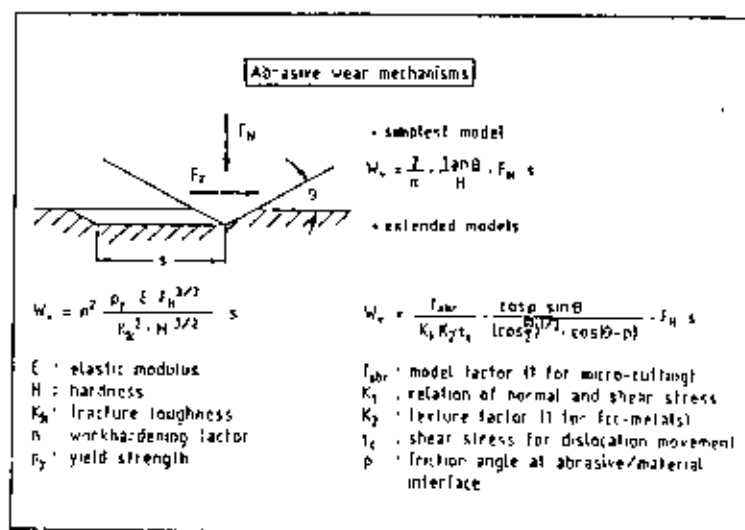


Fig. 2.8 Characteristics of abrasive wear models.

The adhesive wear processes are initiated by the interfacial adhesive junctions which form if solid materials are in contact on an atomic scale. Depending on the nature of the solids in contact different adhesive junctions may result. The whole chain of events which lead to the generation of wear particles is summarised in Fig. 2.9. It is obvious that a number of properties of the contacting solids influence the adhesion wear mechanisms. Since both adhesion and fracture are influenced by surface contaminants and the effect of the environment, it is quite difficult to relate adhesive wear processes with elementary bulk properties of materials.

As is known from the mechanical behaviour of bulk materials under repeated mechanical stressing, microstructural changes in the material may occur which result in gross mechanical failure. Similarly under repeated tribological loading, surface fatigue phenomena may occur leading finally to the generation of wear particles. These effects are mainly based on the action of stresses in or below the surfaces without needing a direct physical solid contact of the surfaces under consideration. The main properties of materials relevant to surface fatigue are listed in Fig. 2.10.

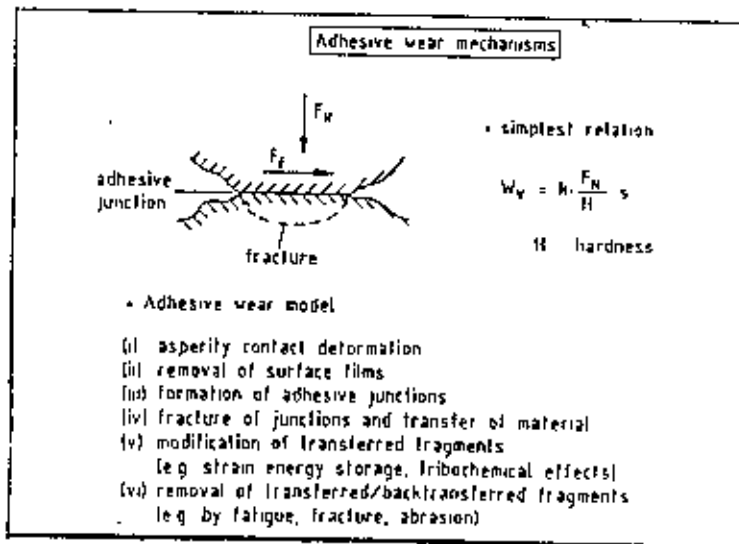


Fig. 2.9 Characteristics of adhesive wear models.

Whereas the mechanism of surface fatigue and abrasion can be described mainly in terms of stress interactions and deformation properties, in tribochemical wear as third partner, the environment and the dynamic interactions between the material components and the environment determine the wear processes. (Fig. 2.11). These interactions may be expressed as cyclic stepwise processes :

i) At the first stage the materials surfaces react with the environment. In this process reaction products are formed on the surfaces.

ii) The second step consists of the attrition of the reaction products as a result of crack formation and abrasion in the contact process interactions of the materials. When this occurs "fresh", i.e. reactive surface parts of the materials are formed and stage (i) continues.

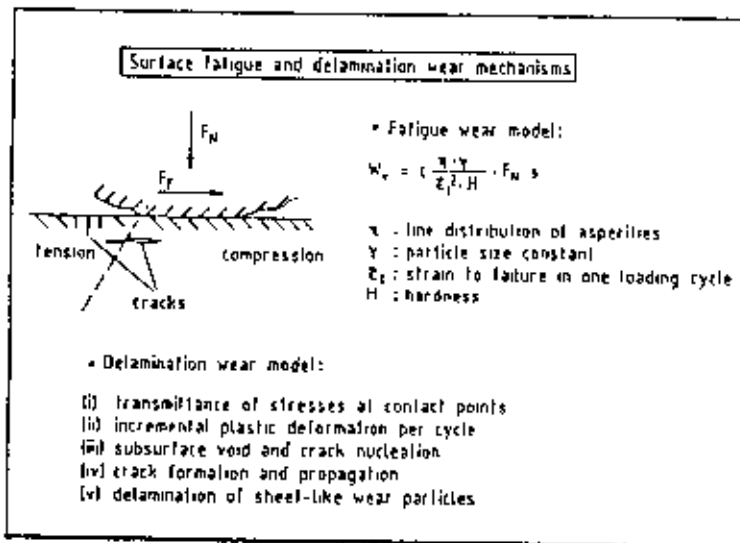


Fig. 2.10 Characteristics of surface fatigue and delamination wear models.

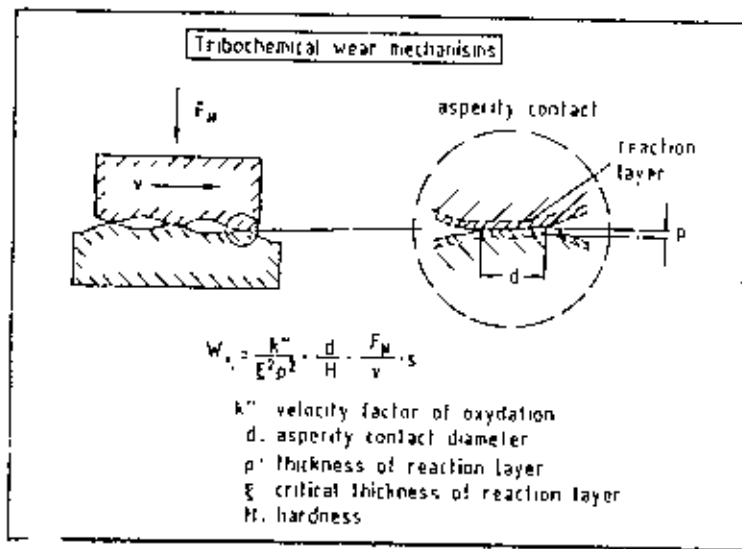


Fig. 2.11 Characteristics of tribochemical wear models.

Wear in steels depends on a number of factors including composition, structure, surface finish, operating conditions and environment. In an ideal situation where material properties and operating conditions remain constant, wear coefficients may be defined which relate to particular causes of wear. However in most practical cases wear rates are controlled by changes in surface properties or the development of surface layers during wear.

The general pattern of behaviour of dry wear in steels was studied by Welsh⁵². He measured wear as a function of load and sliding speed using crossed cylinder tests with 0.52% C steel and found two transitions in the wear rate (Fig. 2.12). Over a wide range of load (0.5 to 400 N) and sliding speed (0.017 to 2.66 m.s⁻¹) the wear process at equilibrium was either of a severe type, producing coarse metallic debris or of a mild type, producing fine oxidised debris. A number of other workers, e.g. Sexton and Fischer⁵³ have confirmed that for dry wear of steels at low load or sliding speed the wear debris is predominantly iron oxide. Fein and Randall⁵⁴ found the same to be true in a hydrocarbon lubricated four ball test. Under these conditions an oxide film is maintained on the surface of the sliding components and provides sufficient lubrication to prevent seizure. A

regime of mild wear is sustained until the point T_1 is reached when the wear rate of the oxide film is sufficient to expose bare metal. At this point metal-to-metal adhesion occurs and a period of severe wear follows. As the load or sliding speed are increased still further, frictional heating causes a rapid increase in the growth rate of the oxide film which is again able to act as a barrier to metal-to-metal adhesion. The curve then undergoes a second transition, T_2 , back to mild wear. Furthermore, studies by Kerridge⁶⁰, using a pin-on-ring test, showed that in the mild wear regime below T_1 , material transfer was involved. Using a tool steel pin and a hardened steel ring he was able to demonstrate that wear debris was formed in a two-stage process:

- 1) material transferred from the pin formed a film on the ring and
- 2) on reaching a critical thickness, wear debris began to be released from the transferred film. At equilibrium the rate of production of wear debris was equal to the rate of transfer of material from the pin

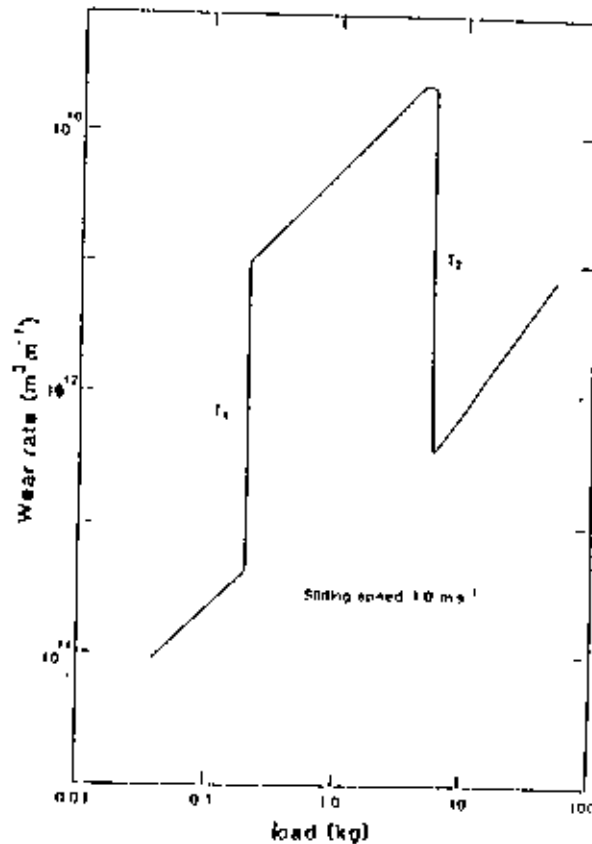


Fig. 2.12 Wear rate as a function of load for like-on-like crossed cylinder tests of 0.52% carbon steel.

Examination of wear debris and worn components using techniques such as SEM and Auger spectroscopy provides information on wear processes and data from which empirical relationship for wear rates may be derived. The action of abrading particles depends strongly on the relative hardness of the material and the abrasive. For relatively ductile materials plastic deformation controls material removal while fracture mechanisms predominate in brittle materials as shown in Fig. 2.13.

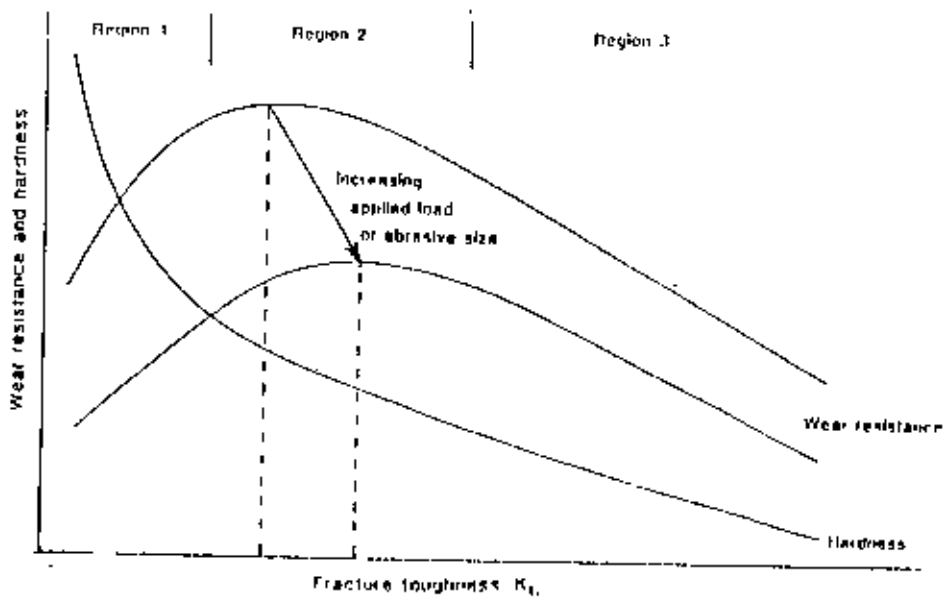


Fig. 2.13 Schematic relationship between wear resistance, hardness and fracture toughness.

A wide range of techniques are employed to reduce wear in machine tools and engineering components. Coatings are applied to increase surface hardness, to reduce adhesion, lower friction or provide a barrier to corrosive attack. Thin coatings require adequate support by the substrate and must be sufficiently ductile to conform under load to local changes in surface profile to optimise surface properties such as friction and hardness and to provide a barrier to corrosive attack.

2.6 Structure and properties of thermally prepared commercial iron-carbon based alloys

A study of the constitution and structure of all steels and irons must first start with the iron-carbon equilibrium diagram. Many of the basic features of this system (Fig 2.14) influence the behaviour of even the most complex alloy steels. For example, the phases found in the simple binary Fe-C system persist in complex steels, but it is necessary to examine the effects of alloying elements have on the formation and properties of these phases.

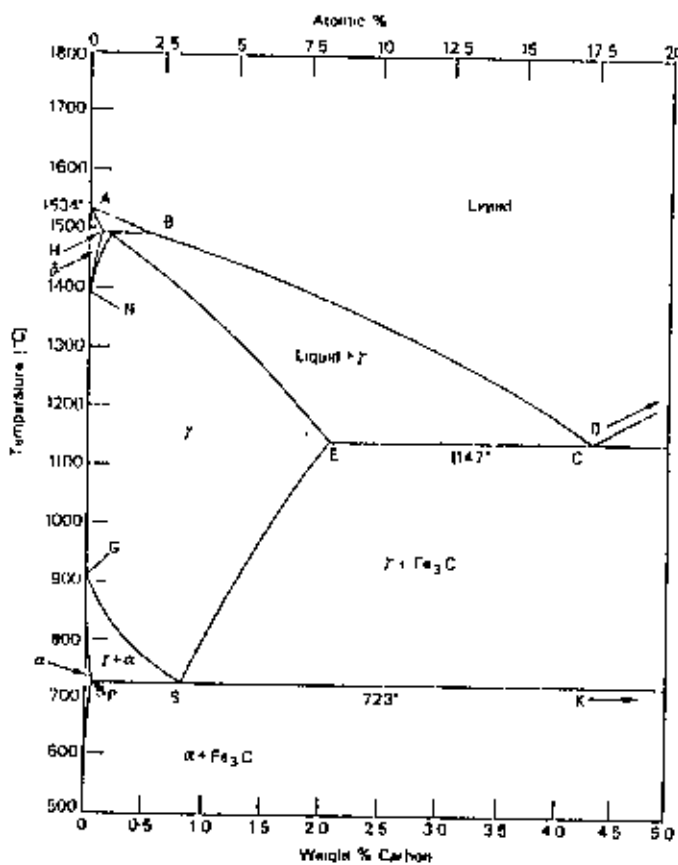


Fig. 2.14 The iron-carbon-carbide equilibrium diagram.

The three phases, ferrite, cementite and pearlite are the principle constituents of the microstructure of plain carbon steels, provided they have been subjected to relatively slow cooling rates to avoid the formation of metastable phases. Effects of carbon and heat treatment on the properties of plain carbon steels is given in Fig. 2.15. Rapid quenching of austenite to room temperature often results in the

formation of martensite. Unlike ferrite or pearlite, martensite forms by a sudden shear process in the austenite lattice which is not normally accompanied by atomic diffusion. Ideally, the martensitic reaction is a diffusionless shear transformation, highly crystallographic in character, which leads to a characteristic lath or lenticular microstructure. The martensitic reaction in steels is the best known of a large group of transformations in alloys in which the transformation occurs by shear without change in chemical composition⁵⁶.

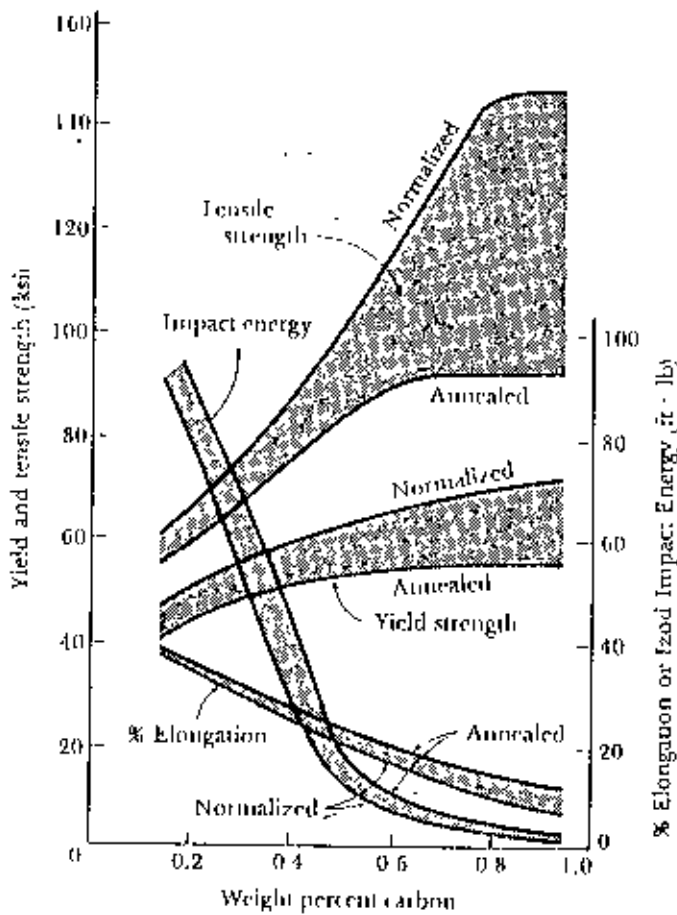


Fig. 2.15 The effect of carbon and heat treatment on the properties of plain carbon steels.

Martensite has a body-centered tetragonal (bct) structure, a distorted form of bcc iron. The tetragonality, measured by the ratio between the axes c/a , increases with carbon content:

$$c/a = 1 + 0.045 \text{ wt \%C}$$

implying that at zero carbon content the structure would be bcc, free of distortion. The effect of carbon on the lattice parameter of austenite, and on the c and a parameters of martensite is shown in Fig. 2.16.

It is interesting to note that carbon in interstitial solid solution expands the fcc iron lattice uniformly, but with bcc iron the expansion is nonsymmetrical giving rise to tetragonal distortion. To understand this important difference in behaviour, it is necessary to compare the interstitial sites for carbon in the two lattices. In each case, carbon atoms occupy octahedral sites, indicated for martensitic in black in Fig. 2.17, and have six near-neighbour iron atoms. In the fcc lattice the six atoms around each interstitial carbon atoms form a regular octahedron, whereas in the bcc case the corresponding octahedra are not regular,

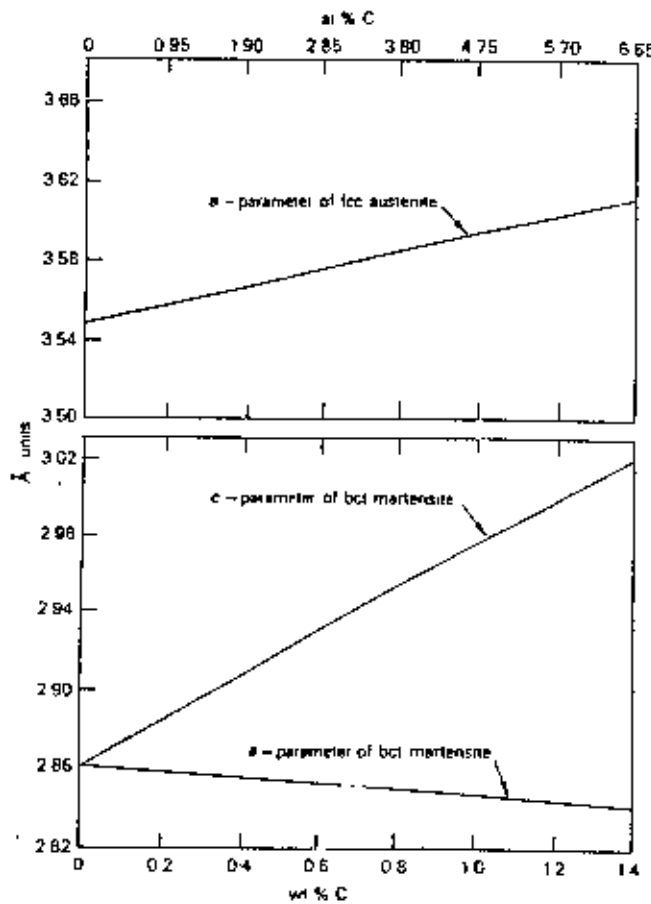


Fig. 2.16 Effect of carbon on the lattice parameters of austenite and of martensite.

being shortened along the z-axis. These compressed octahedra only have four-fold symmetry along the shortened axis in each case, in contrast to the fcc structure in which the regular octahedra have three four-fold axes of symmetry.

Analysis of the distortion produced by carbon atoms in the several types of site available in the fcc and bcc lattices, has shown that in the fcc structure the distortion is completely symmetrical, whereas in the bcc one interstitial atoms in z positions will rise much greater expansion of iron-iron atom distances than in the x and y positions. Assuming that the fcc \rightarrow bcc tetragonal transformation occurs in a diffusionless way, there will be no opportunity for carbon atoms to move, so those interstitial sites already occupied by carbon will be favoured. Since only the z sites are common to both the fcc and bcc lattices, on transformation there are more carbon atoms at these sites causing the z-axis to expand, and the non-regular octahedron becomes more regular. This is largely a unidirectional distortion which leads to the bc tetragonal lattice, the z axis now corresponding to the c-axis in the tetragonal lattice.

Therefore, the tetragonality of martensite arises as a result of interstitial solution of carbon atoms in the bcc lattice, together with the preference for a particular type of octahedral site imposed by the diffusionless character of the reaction.

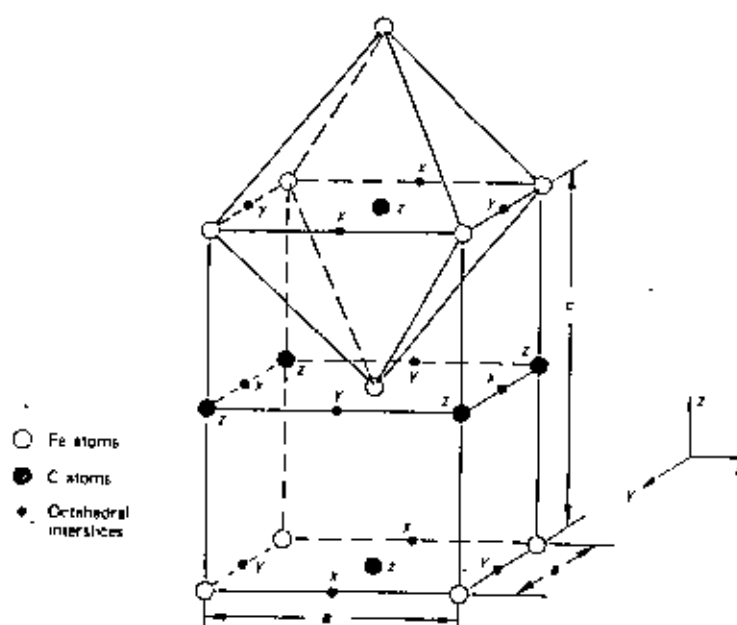


Fig. 2.17 Martensite body-centred tetragonal lattice illustrating the three sets of octahedral interstices

The question of the origin of the high strength of martensite is a difficult one, compounded by the complexity of the structure, a tetragonal lattice with interstitial carbon in solid solution, formed by shear which leads to high densities of dislocations and fine twins. There are, as a result, several possible strengthening mechanisms:

- (1) substitutional and interstitial solid solution
- (2) dislocation strengthening, i.e. work hardening
- (3) fine twins
- (4) grain size
- (5) segregation of carbon atoms
- (6) precipitation of iron carbides

The interstitial solid solution of carbon which results in the tetragonality of martensite is a prime candidate for the role of major strengthening factor.

Martensite is normally very brittle so it is modified by heat treatment in the range 150-700°C by a process called tempering. During tempering carbon is rejected in the form of finely divided carbide phases. The end result of tempering is a fine dispersion of carbides in an α -iron matrix which often bears little structural similarity to the original as-quenched martensite.

On reheating as-quenched martensite, the tempering takes place in four distinct but overlapping stages:

Stage 1, up to 250°C — precipitation of ϵ -iron carbide; partial loss of tetragonality in martensite.

ϵ -iron carbide has a close-packed hexagonal structure, and precipitates as narrow laths on cube planes of the matrix with a well-defined orientation relationship⁵⁶:

$$\{101\}_{\alpha'} // \{1011\}_{\epsilon}$$

$$\{011\}_{\alpha'} // \{0001\}_{\epsilon}$$

$$[111]_{\alpha'} // [1210]_{\epsilon}$$

In the higher carbon steels, an increase in hardness has been observed on tempering in the range 50-100°C, which is attributed to precipitation hardening of the martensite by ϵ -carbide.

Stage 2, between 200 and 300⁰C — decomposition of retained austenite to bainitic ferrite and cementite, but no detailed comparison between this phase and lower bainite has yet been made.

Stage 3, between 200 and 350⁰C — replacement of ϵ -iron carbide by cementite; martensite loses tetragonality

Due to the formation of cementite the matrix loses its tetragonality and becomes ferrite. The relationship is that due to Bagaryatski:

$$(211)_{\alpha'} // (011)_{\text{Fe}_3\text{C}}$$

$$[011]_{\alpha'} // [100]_{\text{Fe}_3\text{C}}$$

$$[111]_{\alpha'} // [010]_{\text{Fe}_3\text{C}}$$

This reaction commences as low as 100⁰C and is fully developed at 300⁰C, with particles up to 200 nm long and ~15 nm in diameter. During tempering, the most likely sites for the nucleation of the cementite are the ϵ -iron carbide interfaces with the matrix and as the Fe_3C particles grow, the ϵ -iron carbide particles gradually disappear.

The twins occurring in the higher carbon martensites are also sites for the nucleation and growth of cementite which tends along the twin boundaries forming colonies of similarly oriented lath-shaped of $\{112\}_{\alpha}$ habit plane.

A third site for the nucleation of cementite is the grain boundary regions, both the interlath boundaries of the martensite and the original austenite grain boundaries. There is some evidence to show that these grain boundary cementite films can adversely affect ductility. However, they can be modified by addition of alloying elements.

Stage 4, above 350⁰C — cementite coarsens and spheroidizes by losing crystallographic morphology; recrystallization of ferrite.

The coarsening of cementite commences between 300⁰C and 400⁰C, while spheroidization takes place increasingly up to 700⁰C. At the higher end of this temperature the martensite lath boundaries are replaced by more equi-axed ferrite grain boundaries by a process which is best described as recrystallization. The final result is an equi-axed array of ferrite grains with coarse spheroidized particles of Fe_3C , partly, but not exclusively, in the grain boundaries.

The original martensite lath boundaries remain stable up to 600°C , but in the range $350\text{--}600^{\circ}\text{C}$, there is considerable rearrangement of the dislocations within the laths and at those lath boundaries which are essentially low angle boundaries. This leads to a marked reduction in the dislocation density and to lath-shaped ferritic grains closely related to the packets of similarly orientated laths in the original martensite. This process, which is essentially one of recovery, is replaced between 600 and 700°C by recrystallization which results in the formation of equi-axed ferrite grains with spheroidal Fe_3C particles in the boundaries and within the grains. This process occurs most readily in low carbon steels. At higher carbon contents the increased density of Fe_3C particles is much more effective in pinning the ferrite boundaries, so recrystallization is much more sluggish. The final process is the continued coarsening of Fe_3C particles and gradual ferrite grain growth (Fig. 2.18)

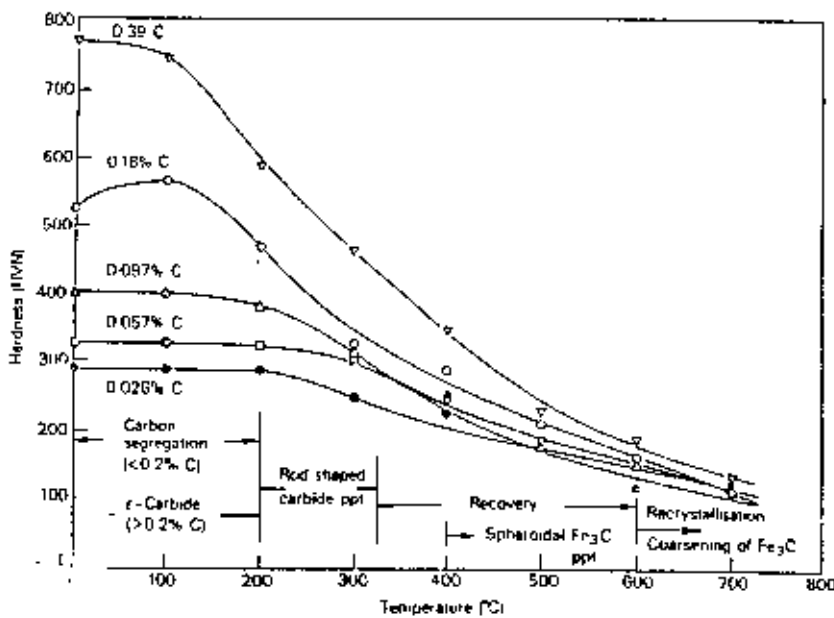


Fig. 2.18 Hardness of iron-carbon martensites tempered 1 h at $100\text{--}700^{\circ}\text{C}$.

Therefore by controlling the factors that affect the martensite reaction and the execution of the quench and temper heat treatment in plain carbon steels, we can control the final properties of the steel. The effect of tempering temperature on the mechanical properties of plain carbon steel is given in Fig. 2.19.

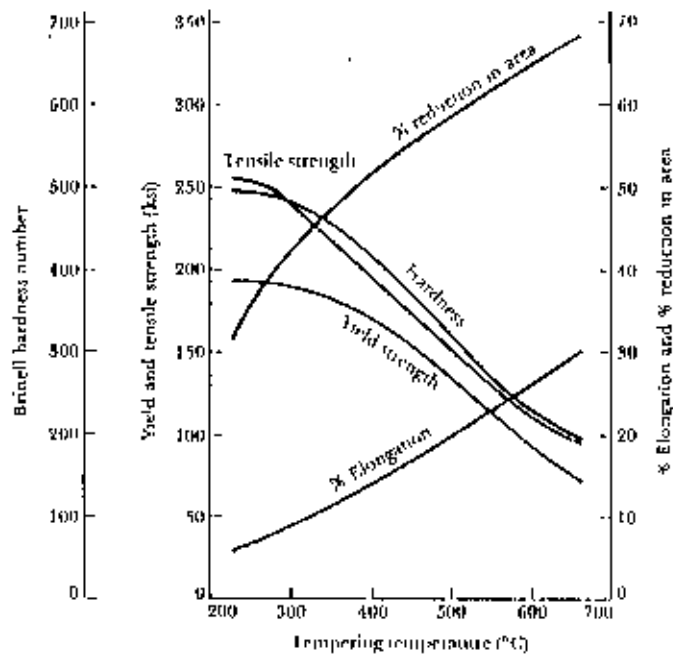


Fig. 2.19 The effect of tempering temperature on the mechanical properties of plain carbon steel.

3. EXPERIMENTAL

3.1 Electroplating

3.1.1 Substrate and its pretreatment

Mild steel substrates were used throughout the study. The dimensions of the substrate used for different tests are given in Table 3.1. The substrates after being cut into desired dimension were pretreated through different steps in order to get a clean surface ready for electrodeposition. A flow chart showing the sequence of steps is given below,

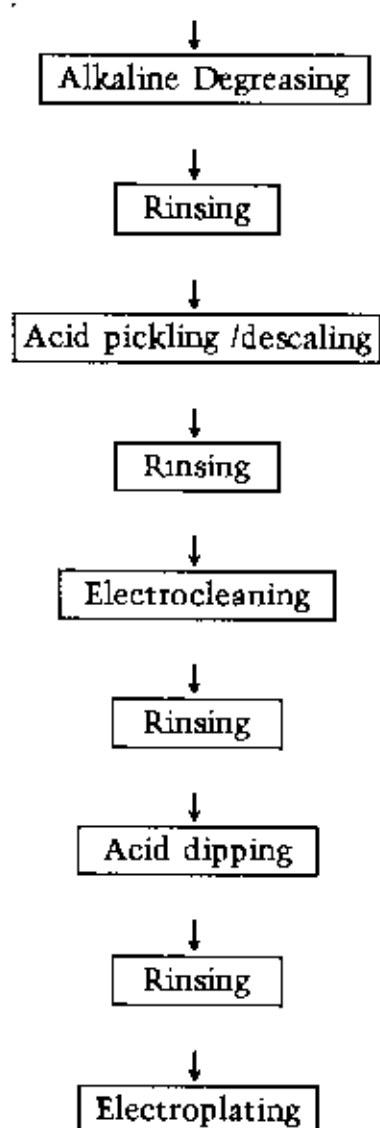


Fig 3.1 Flow chart of pretreatment operations applied to substrate before electrodeposition.

Alkali degreasing : Degreasing is an operation which removes soils that do not readily react with acid, such as grease, oil, soaps, lubricants and carrier coatings and therefore alkali degreasing is often done before pickling or descaling. Degreasing was carried out by dipping the substrate in the alkaline solution (Table 3.2).

Descaling : Acid pickling or descaling was done by immersing the substrate in an aqueous acid solution (Table 3.2) in order to obtain the chemical removal of scale present on mild steel surface, thereby making the substrate rustfree. Details of pickling operation are given in Table 3.2.

Table 3.1 Size of substrate used in different investigations.

Material	Substrate Area	Name of Investigation
M.S. sheet	50 mm x 30 mm x 2.5 mm	Hardness & Metallography
M.S. sheet	60 mm x 30 mm x 0.1 mm	Chemical analysis
M.S. sheet	150 mm x 60 mm x 1 mm	Bend test
M.S. rod	60 mm length, 8 mm dia	Wear test

Electrocleaning : Electrocleaning is used as a means of increasing the rate of descaling. The electrocleaning solution was the same as degreasing solution (Table 3.2). The substrate was used as anode and the stainless steel having the same dimension of the substrate as cathode. This treatment removes metallic smuts and prevents the deposition of other positively charged metallic ion which otherwise may result in a detrimental film on the substrate.

Acid dipping : This operation is applied to neutralise any residual alkali film or to remove the light oxide films or to activate the substrate surface just before electrodeposition

Rinsing : Substrate surface is rinsed with distilled water between every operational stage to expel the chemicals of the bath previously used and to avoid the contamination of the subsequent bath.

Table 3.2 Particulars of substrate pretreatment operation.

Name of the operation	Reagents used g/l	Operating Conditions		
		Current Density mA/cm ²	Temperature °C	Time
Alkaline degreasing	NaOH : 50 Na ₂ CO ₃ : 24 NaSiO ₃ : 20 Na ₅ P ₃ O ₅ : 5	55	70	30 min.
Pickling	H ₂ SO ₄ : 20 H ₂ O : 80		70	5 min.
Electrocleaning	Same as alkaline degreasing		60	2 min.
Acid dipping	HCl : 10 H ₂ O : 90		Room	15 sec.

3.1.2 Electroplating set-up

Electrodeposition was carried out in a conventional cell with vertical electrode arrangement. The cell consisted of a 400 ml glass beaker, a D.C. source, a magnetic stirrer, a perspex sheet and electrode holders.

Prior to Fe-C and Fe-Ni-C alloy deposition, the substrates were lacquered on one side so as to expose a predetermined area to the plating solution.

The beaker containing the electroplating solution was placed on the magnetic hot plate and agitated by a magnetic stirrer to have complete dissolution and mixing of the bath salts. Specimens for bend test requiring a larger area were plated in a beaker containing 2000 ml of plating solution. The anode and cathode were connected to the D.C. power supply via a milliammeter. A mild steel sheet was used as anode throughout the study and had the same dimension as cathode. In the case of cylindrical substrate used for wear tests, three anodes

were arranged around the substrate to achieve uniformity in current distribution. A Schematic diagram of the experimental set-up is shown in Fig.3.2.

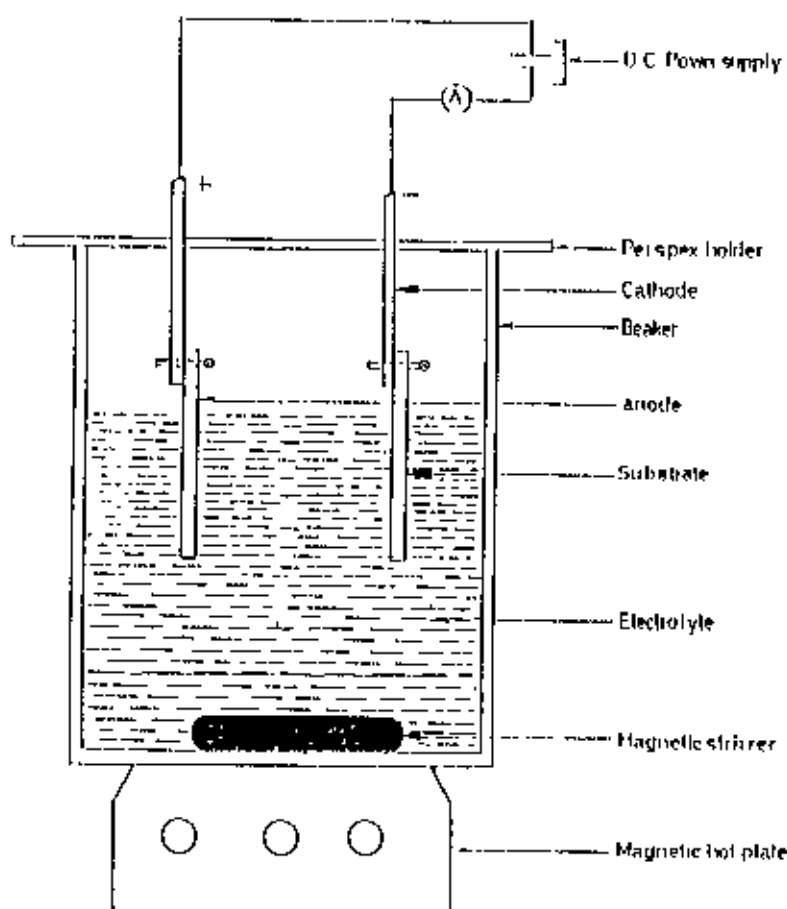


Fig 3.2 Schematic diagram of electrodeposition set-up.

3.1.3 Preparation of Fe-C and Fe-Ni-C alloy coatings

Electrodeposition of Fe-C and Fe-Ni-C alloy was carried out galvanostatically at room temperature from sulphate based baths. All baths contained 150 g/l ferrous sulphate. Amount of citric acid (CA) and L-Ascorbic acid (LAA) in the baths was varied. Details of various bath composition are given in Table 3.3. Iron-nickel-carbon alloy was deposited from baths which contained 20-50 g/l nickel sulphate. Pure iron was deposited in a bath containing only 150 g/l ferrous sulphate.

Table 3.3 Composition of different baths used in the deposition of Fe-C and Fe-Ni-C alloys.

Bath Designation	FeSO ₄ , 7H ₂ O g/l	Citric Acid C ₆ H ₁₀ O ₈ g/l	L-Ascorbic Acid C ₆ H ₈ O ₆ g/l	NiSO ₄ , 6H ₂ O g/l	Gelatin g/l	Sodium Lauryl Sulphate g/l
A	150	—	—	—	—	—
B		10	10	—	—	—
C		1.5	1.5	—	—	—
D		0.5	0.5	—	—	—
E		10	10	50	—	—
F		10	10	20	—	—
G		10	10	—	1	—
H		10	10	—	0.2	—
I		10	10	—	0.2	0.5

After preparing the set-up, electrodeposition was started by connecting the substrate or cathode to the negative terminal and the anode to the positive terminal of a D.C. source. Deposition was carried out at constant current density 40 mA/cm² for 1 hr.

After deposition the samples were thoroughly rinsed with distilled water to remove surplus electrolyte, then dried in hot air and stored in a dessicator for subsequent investigations.

3.2 Chemical analysis

For chemical analysis of Fe-C and Fe-Ni-C alloy, the samples were bent or buckled to strip off the coating from the substrate after deposition. Then, 0.5g samples were taken for carbon and nickel analysis. Carbon content of Fe-C and Fe-Ni-C alloy deposit was determined by the combustion method using Strohleim apparatus⁵⁷.

Nickel content of iron-nickel-carbon alloy was determined by the conventional wet method using di-methyl glyoxime⁵⁷. The coating was first dissolved in diluted HCl solution and heated. At neutral point, dimethyl glyoxime ($C_4H_8N_2O_2$) was added. Ni-glyoxime precipitate of blood red colour was formed which was separated by filtering through a dual filter paper of equal weight. The filtrate was treated several times with NH_4OH dimethyl glyoxime in sequence until precipitation was completed. The precipitation was then washed several times with hot water, dried in a oven $110-120^0C$ for 1 hr. and weighed as $NiC_3H_{14}O_4N_4$.

3.3 Optical microscopy

For metallography, samples were cut into small pieces at right angles to the coated surface. Then the cross-section of the specimens were made parallel by a grinding machine and mounted cross sectionally with bakelite powder. Then the samples were polished by standard metallographic techniques and etched in 2% nital solution (2 ml HNO_3 and 98 ml ethyl alcohol). The microstructure of the samples was examined under an optical microscope and the micrographs of the microstructure were taken.

Metallography was done on as deposited and annealed samples. Deposition was done in a bath containing 150 g/l ferrons sulphate and 10 g/l citric acid (CA) and 10 g/l L-Ascorbic acid. as-deposited. Annealing was carried out by holding the as-deposited sample in lead bath for 25 min. at $850^0 C$ followed by furnace cooling. Optical microscopy was also done on bent samples and on wear test samples to find out the bending cracks and wear phenomenon respectively. Wear test debris were also investigated by optical microscopy, because the geometry and nature of the wear debris can give an indication of the principal wear mechanism in operation.

3.4 X-ray diffraction

X-ray diffraction pattern of as deposited, annealed and tempered martensitic Fe-C alloy was taken to determine the phases and to compare it with thermally produced Fe-C phases. The operating condition of X-ray diffractometer is shown in Table 3.4.

Table 3.4 Operating conditions of X-ray diffractometer.

Radiation	CuK α
Voltage and current	30 KV, 15 mA
Scanning speed	2 $^{\circ}$ /min., 1/2 $^{\circ}$ /min.
Chart speed	10 mm/min., 2.5mm/min
Range	10 $^{\circ}$ to 90 $^{\circ}$, 40 $^{\circ}$ to 90 $^{\circ}$

3.5 Differential thermal analysis

Thermal analysis studies are concerned with measurement of heat and weight changes in a system when it is heated or cooled in a predetermined manner. They provide insight into the physical nature of the system, mineralogical make up and the chemical reactivity in a given environment and behaviour during heating e.g. phase change, reactions etc.

In DTA, two small crucibles, one containing an inert reference substance like alumina and the other containing the test sample are placed close together in a furnace and heated at a given rate. There is a thermocouple in close contact with each to sense temperatures. During heating, a suitable device records the temperatures, of the test sample as well as the temperature difference between the sample and the reference ($T_S - T_R$). Up to a very high temperature, no heat changes occur in alumina. Therefore, if at a temperature an exothermic reaction occurs in the test sample, the differential temperature ($T_S - T_R$) rises. Once the reaction is over, ($T_S - T_R$) must again decay to a zero value. One thus obtains an exothermic peak. For an endothermic reaction the situation is reversed. Fig. 3.3 shows schematically the DTA plots thus obtained.

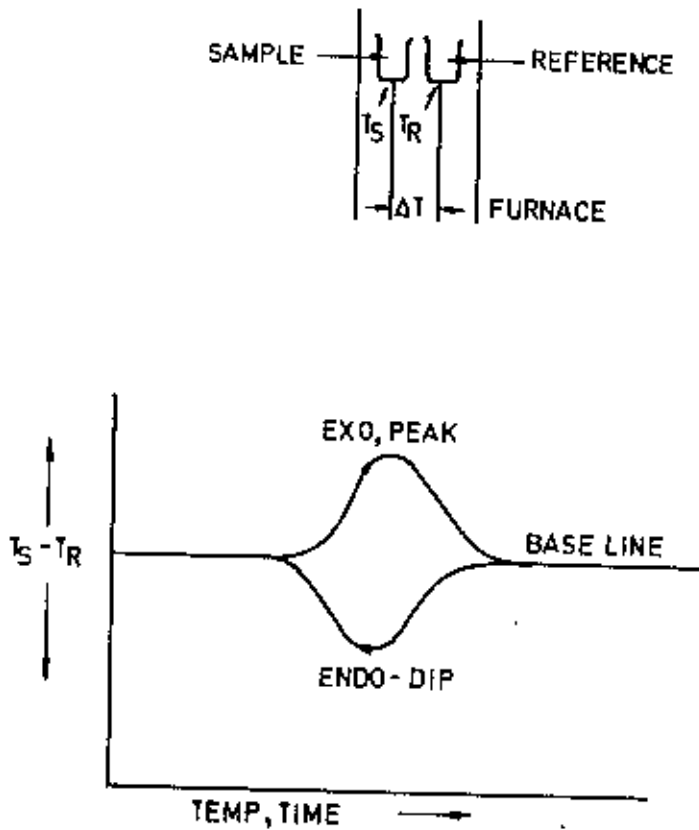


Fig. 3.3 Schematic diagram showing DTA set-up and DTA plots.

In this study, differential thermal analysis of the as-deposited Fe-C alloy and annealed file steel samples were made using Rigaku Thermal Analyser TAS 100 with basic unit TG 8110. For each case 0.5 g samples were taken. The samples were heated in an inert atmosphere and the rate of heating used was 15°C per minute. The maximum temperature was raised to 1000°C . The results were recorded on a X-Y-t recorder.

3.6 Mechanical properties

3.6.1 Microhardness measurement

Microhardness values were determined by using a Shimadzu Microhardness Tester. Microhardness measurements were carried out with a 50 g load for 5 seconds on polished and unetched Fe-C and Fe-Ni-C alloy coatings. The as-deposited samples were dark under microscope and therefore microhardness measurements on the surface was difficult. So, polishing and cleaning were done with a 4/0 emery paper and acetone respectively to make the deposited surface bright and to measure the diagonal length of the indentation easily.

Microhardness measurements were taken on as deposited and tempered samples obtained from various baths. Tempering was done in an oven at 200°C for 1/2 hr. In this study, low tempering temperature was selected because the temperatures and the periods of heating required to bring the structure of electrodeposited, supersaturated alloys to equilibrium are lower than those required for non-equilibrium thermal alloys⁵⁸.

3.6.2 Bend test

For bend test samples, deposition was carried out at 40 mA/cm² to a constant thickness of 25 µm. To determine ductility of coating bend test was carried out following the ASTM B489-68 standard⁴⁸. Bending specimens of size 150 mm long and 10 mm wide were cut by a Guillotine shear machine from the middle portion of the electrodeposited sample.

A series of mandrels with diameters from 6 to 50 mm in 3 mm steps with length of 150 mm were used for the test. At first 33 mm dia mandrel was taken and fixed in a vise. Then the test specimen, with coating outward, was bent over the mandrel so that as the bend progresses the test specimen will remain in contact with the top of the mandrel. Bending was continued with slow, steadily applied pressure until the two legs were parallel. If there were no cracks visible under a

20X magnifier, the test was repeated, using new specimen on progressively smaller-diameter mandrels until cracks appeared across or through the plating. The preceding mandrel diameter was taken as the value for the ductility determination. The elongation is determined as follows :

$$E = 100T/(D+T)$$

where,

E = percentage elongation

T = total thickness of the basis metal and deposit, and

D = diameter of the mandrel

Bend test was carried out on both as-deposited and tempered samples. Tempering was done instantly after deposition in an oven at 200°C for 1/2 hr.

3.6.3 Wear test

For wear test, deposition was carried out on cylindrical mild steel specimen for 1/2 hr. at a current density of 40 mA/cm² to get a coating thickness of 20µm. It was found that coating thickness on the cylindrical rod was almost doubled than that on the flat plate for a certain period of deposition. The cylindrical pins of 8 mm dia and 6.5 mm length were cut from the coated samples and the sharp edges of the specimens were rounded with a 2/0 emery paper for good contact with counter body during wear testing. Before the test, both the pin and the counter body were cleaned with acetone.

Wear test were carried out in a pin-on-disc type apparatus (Fig.3.4) under dry sliding condition at room temperature. Grey cast iron discs of 80 mm diameter and about 10 mm thickness were used as the counter body. During wear test, the sample was pressed against the rotating disc under a constant load for a specified time. Loads of 1000 g, 500 g, 250 g were used and the testing periods were 5, 10 and 15 minutes. The counter body was rotated at 500 rpm which gave a linear speed of 1.39 m/s.

After the test the worn samples of the pins were examined under an optical microscope and the width of the wear scar was measured. At least three tests were carried out for each set of conditions and the average width of wear scar on the coated pin was taken as a measure of the coating wear.

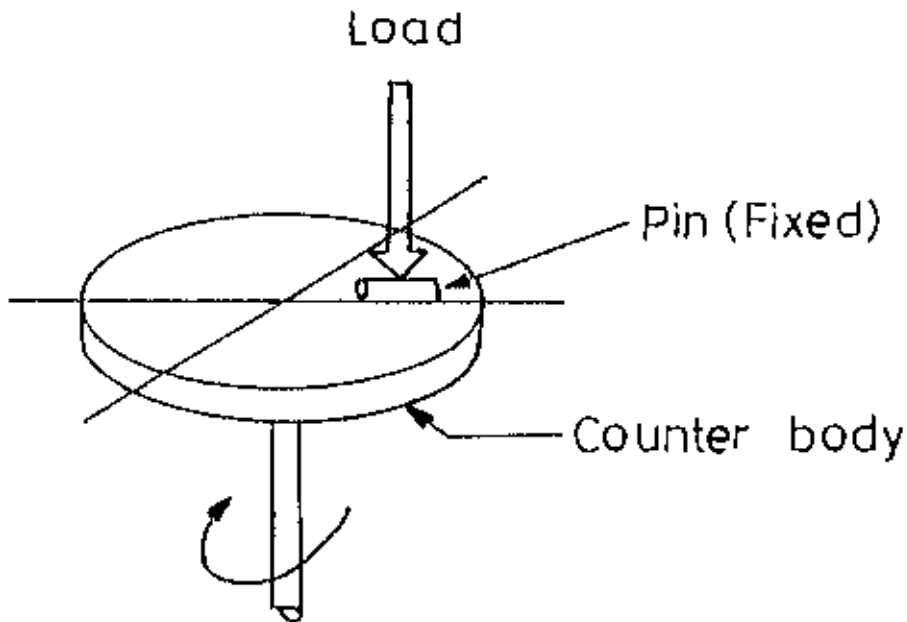


Fig. 3.4 Schematic diagram of pin-on-disc type wear test apparatus.

In this study wear test was carried out both on as deposited and tempered samples. Tempering was done in an oven at 200°C for 1/2 hr. Bare mild steel pins were also tested for comparison.

4. RESULTS AND DISCUSSIONS

4.1 Characterization of Fe-C and Fe-Ni-C alloy coatings

4.1.1 Chemical composition

The variation of carbon content of the deposit with bath composition is shown in Fig. 4.1. It is seen from the figure that the deposit obtained from the bath containing 10 g/l CA and 10 g/l LAA possesses 1.1 wt% carbon, while the bath containing 1.5 g/l CA and 1.5 g/l LAA gives rise to iron-carbon deposit with 1 wt% carbon. The bath containing 0.5 g/l CA and 0.5 g/l LAA yields a deposit with 0.88 wt% carbon whereas the bath containing 0.2 g/l CA and 0.2 g/l LAA causes an incorporation of 0.56 wt% carbon into the deposit. It is apparent that the carbon content of the deposit becomes less sensitive to CA and LAA content of the bath when CA and LAA are present in higher amounts. Such insensitivity of carbon content of iron-carbon deposit to citric acid content of the bath beyond a certain value was also observed by others⁸.

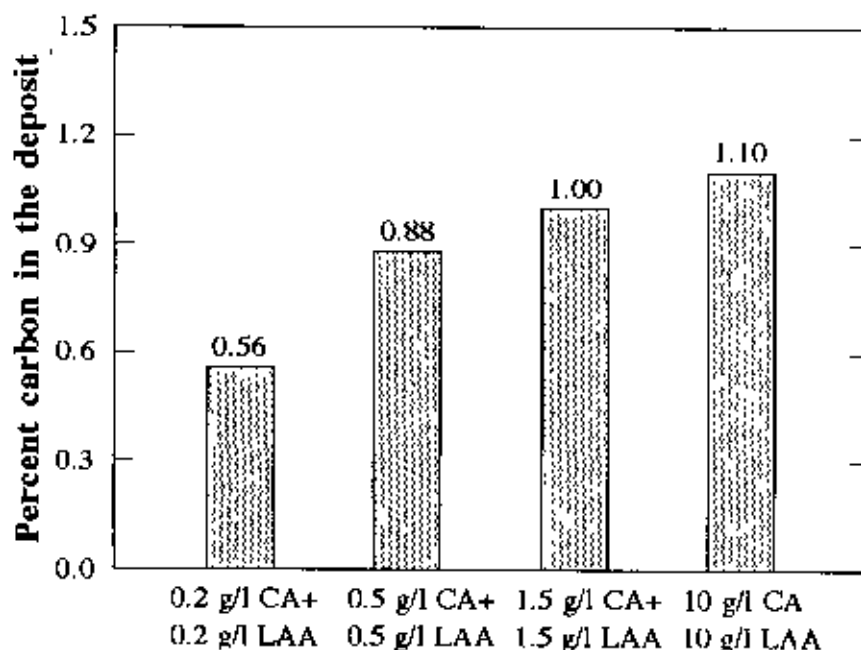


Fig. 4.1 Variation of carbon content of Fe-C alloy deposited from baths containing 150 g/l ferrous sulphate and varying amount citric acid (CA) and L-ascorbic acid (LAA).

The carbon content of the Fe-Ni-C alloy deposited from baths containing various amount of nickel sulphate is shown in Fig. 4.2. Error bars are shown to indicate the spread of experimental data. The carbon content of Fe-Ni-C alloy is found to be about 1.14 wt% when 20 g/l nickel sulphate is added to the bath B (Table 3.3). Bath containing 50 g/l nickel sulphate gives rise to deposits with an average carbon content of 1.27 wt%. Although these data indicate a slight increase in carbon content of the deposit as nickel content of the bath increases, but given the scatter of the data further confirmation is necessary. It is clear, however, that the carbon content of the deposits from nickel sulphate containing baths (Baths E and F) is above 1 wt%, as is the case in deposits from nickel sulphate free bath (Bath B). Presence of nickel sulphate causes an incorporation of nickel into the deposit. Thus baths containing 50 g/l and 20 g/l nickel sulphate yield deposits with 6.3 wt% and 4.3 wt% nickel respectively.

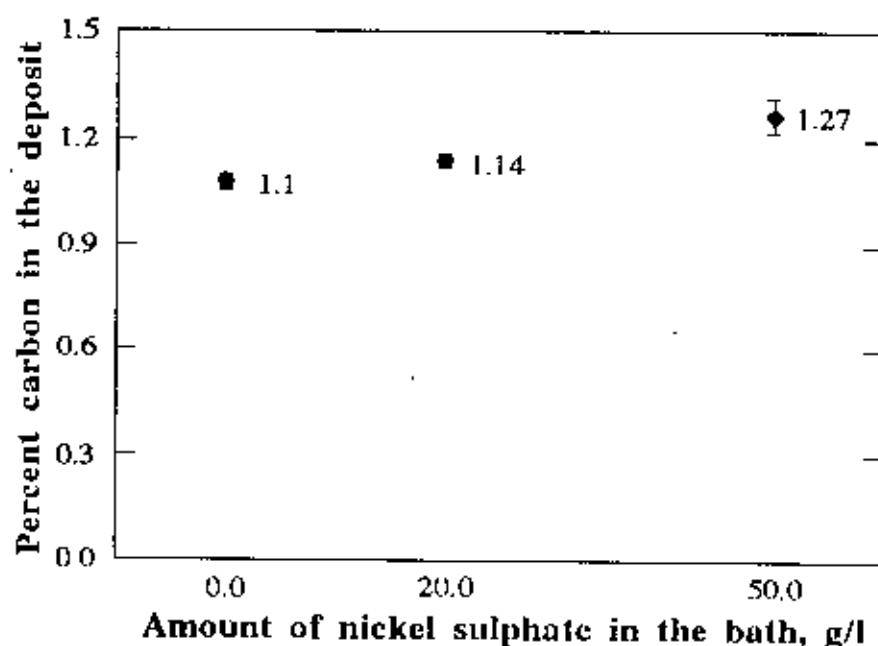


Fig. 4.2 Variation of carbon content of Fe-Ni-C alloy deposited from baths containing 150 g/l FeSO_4 , 10 g/l citric acid and 10 g/l L-ascorbic acid and varying amount of nickel sulphate.

4.1.2. Structure and morphology

Fig. 4.3 shows the cross-sectional micrograph of as-deposited Fe-1.1%C alloy coating from bath containing 10 g/l CA and 10 g/l LAA. The un-etched cross section in Fig. 4.3a shows the coating to be compact and non-porous. However, a number of cracks across the thickness are visible. These cracks are believed to have formed during metallographic sample preparation. Nital etch is seen to darken the as-deposited Fe-1.1%C alloy (Fig. 4.3b). The characteristic acicular martensitic structure found in thermally treated Fe-C alloys is not observed in the electrodeposited sample. This is possibly due to the fact that electrodeposition produces finer structure, some times not revealed by optical microscopy⁵⁸.

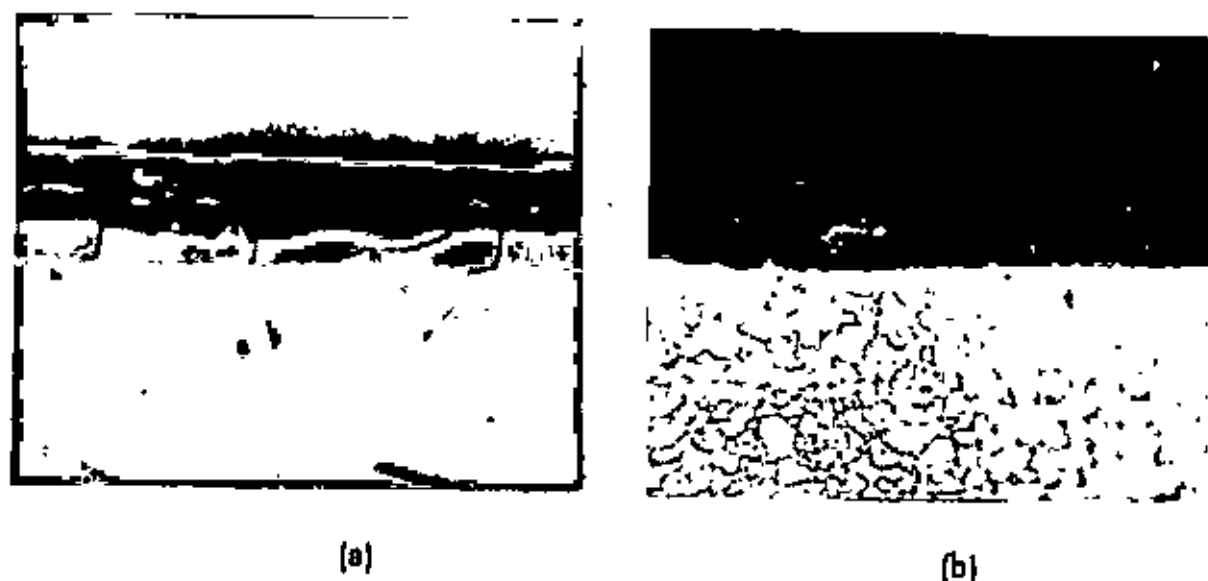


Fig. 4.3 Cross-sectional micrographs of Fe-1.1%C alloy coating.
a) Unetched condition
b) Etched condition (2% nital)

Annealing of the as-deposited Fe-1.1%C alloy was done and its cross-sectional microstructure is shown in Fig. 4.4. Etched cross-section of the annealed Fe-1.1%C coating shows a mixture of pearlite and cementite as is expected in an annealed high carbon steel⁵⁸. The bright layer below Fe-1.1%C alloy coating is a nickel coating used to avoid diffusion of carbon from coating to the substrate during annealing.



Fig. 4.4 Cross-sectional microstructure of annealed Fe-1.1% alloy coating.

The appearance and morphology of the surface of the deposits obtained under various conditions were examined both visually and under a stereoscope. The surface of the as-deposited Fe-1.1%C coating was relatively smooth.[Fig. 4.5a] but dendrites or treeing were observed at the edges of the sample, where high current density is most likely to occur. This dendritic tendency increased with increasing deposition time. These as-deposited samples were somewhat adherent, brittle and crack free. Deposit from 1.5 g/l CA and 1.5 g/l LAA containing bath showed better adherence than the previous ones and the deposit from bath

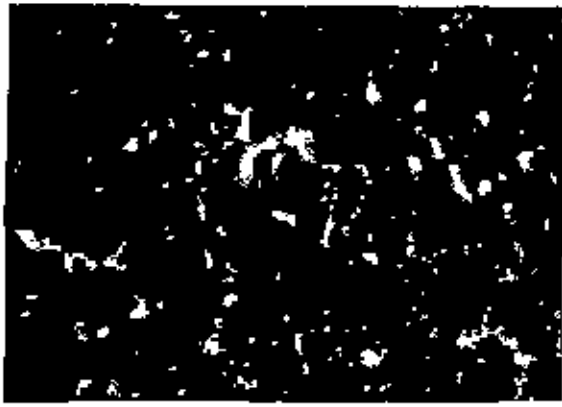
containing 0.5 g/l CA and 0.5 g/l LAA showed maximum adherence, but these deposits were of much lower hardness compared to the deposit from bath containing 10 g/l citric acid and 10 g/l L-ascorbic acid.

The Fe-4.3%Ni-1.1%C alloy coating obtained from nickel sulphate containing bath showed almost the same morphology as that of as-deposited Fe-1.1%C alloy (Fig. 4.5a). However, it was observed that when three to four or more samples were deposited in succession from the same bath, latter deposits showed a stripped type morphology due possibly to hydrogen evolution⁵⁹ (Fig. 4.5b).

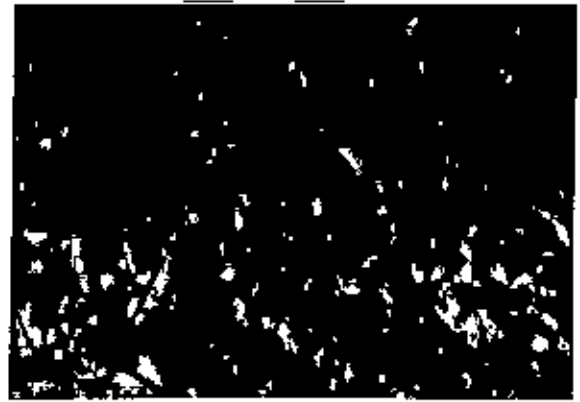
Upon visual examination, deposits from bath containing 0.2 g/l gelatin (Bath H) were found to be bright. Dendrites formed at the edges of the deposits were comparatively lower in amounts and were very fine as compared with those formed on samples obtained from gelatin free baths (Bath B and Bath F). It has been found by others⁶⁰ also that use of 0.2 g/l of gelatin as an additive markedly suppresses the dendritic growth and promotes bright, compact and fine grained deposits. However when examined under stereoscope, deposits from gelatin containing bath showed stripped surface (Fig. 4.5d) which seems to be rougher than the deposit formed without gelatin addition.

When sodium-lauryl-sulphate was added to the gelatin containing bath, its effect on deposit morphology was dramatic. It completely eliminated the stripped surface and provided a smooth coating. But the coating was not bright and showed small pits all over the surface when examined under the stereoscope (Fig. 4.5e). When addition agent is used in the bath, it preferentially adsorbs on the high points of an irregular surface where it acts as an insulator. This inhibits deposition of metal and diverts current to recessed areas⁶¹. In this way it produces smooth surface.

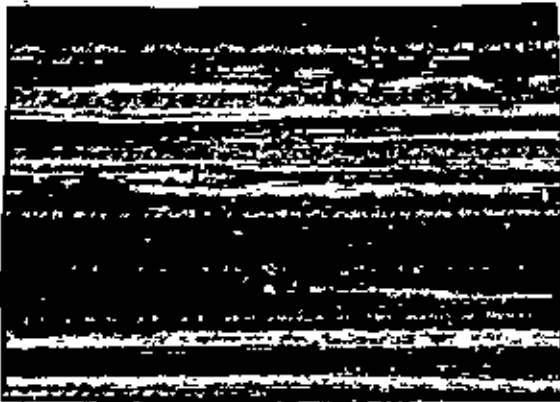
Tempering of the Fe-1.1%C and Fe-4.3%Ni-1.1%C alloy deposit at 200°C for 0.5 hr. produced a network of fine hairline cracks on the surface as shown in Fig. 4.5b. This may be due to the release of residual stresses of the coating which occurred during electrodeposition.



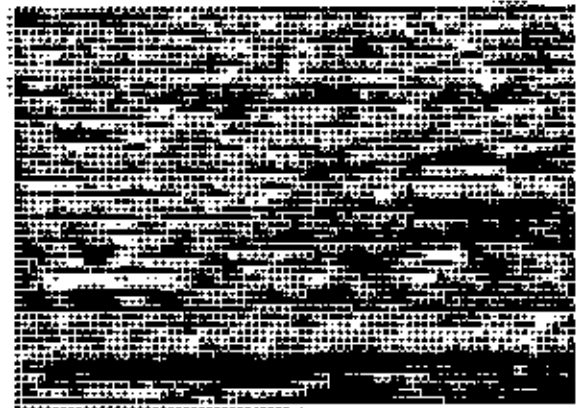
(a)



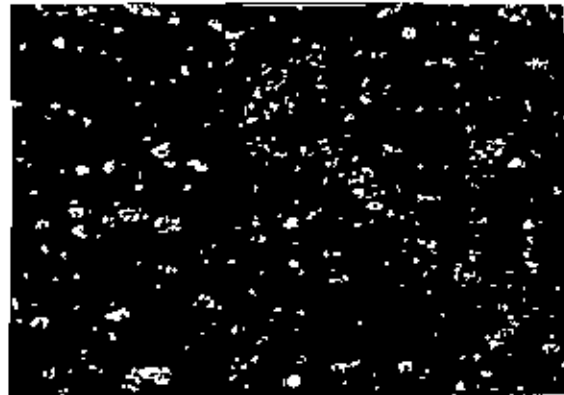
(b)



(c)



(d)



(e)

Fig.4.5 Morphologies of Fe-1.1%C and Fe-4.3%Ni-1.1%C alloy coatings.

a) As-deposited Fe-1.1%C alloy

b) Tempered Fe-1.1%C alloy

c) As-deposited Fe-4.3%Ni-1.1%C alloy

d) As-deposited Fe-1.1%C alloy with gelatin as an additive in the bath

e) As-deposited Fe-1.1%C alloy with gelatin and sodium-lauryl-sulphate as additives in the bath

4.1.3. X-ray diffraction

X-ray diffraction studies were done on as-deposited and tempered Fe-1.1%C alloy obtained from baths containing 10 g/l citric acid and 10 g/l L-ascorbic acid. X-ray diffraction study was also done on a mild steel sheet for comparison. Diffraction pattern of mild steel shows (Fig. 4.6) three prominent diffraction peaks at the 2θ values of 44.6° , 65° and 82.25° . These peaks correspond to (110), (200) and (211) planes of alpha iron respectively.

The as-deposited and tempered Fe-1.1%C alloy show almost the same diffraction patterns as illustrated in Fig. 4.7 and 4.8. Their peak positions are similar to those of alpha iron. Although the peak from (110) plane is prominent, the peaks from (200) and (211) are found to be quite diffuse. Haseeb and Huq⁸ attributed this to the presence of tetragonal lattice of the deposit which is the characteristics of martensitic structure. Ezaki and Enomoto⁶ studied their electrodeposited Fe-1.2%C alloy by X-ray diffraction and found that (200) and (211) peaks obtained from their deposits were also quite diffuse. They showed, through computer simulation, that these peaks actually consist of two doublets

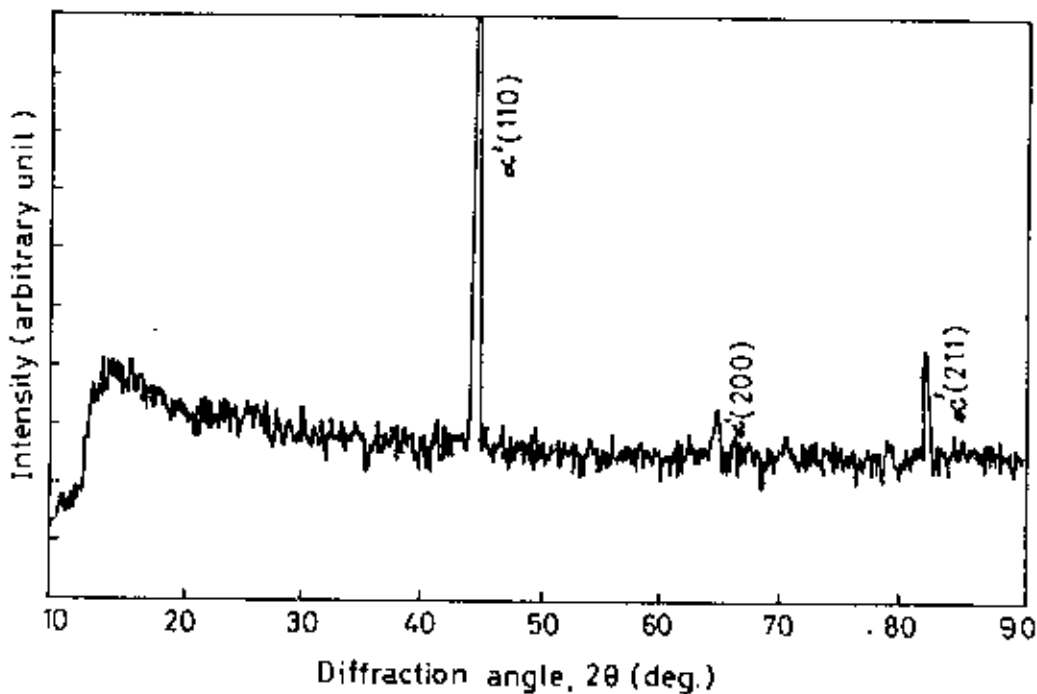


Fig. 4.6 X-ray diffraction pattern of mild steel.

corresponding to tetragonal martensitic structure. They also confirmed the presence of martensitic structure in their deposits by means of transmission electron microscope study. Thus the Fe-1.1%C deposit obtained in this study is also believed to be martensitic in structure.

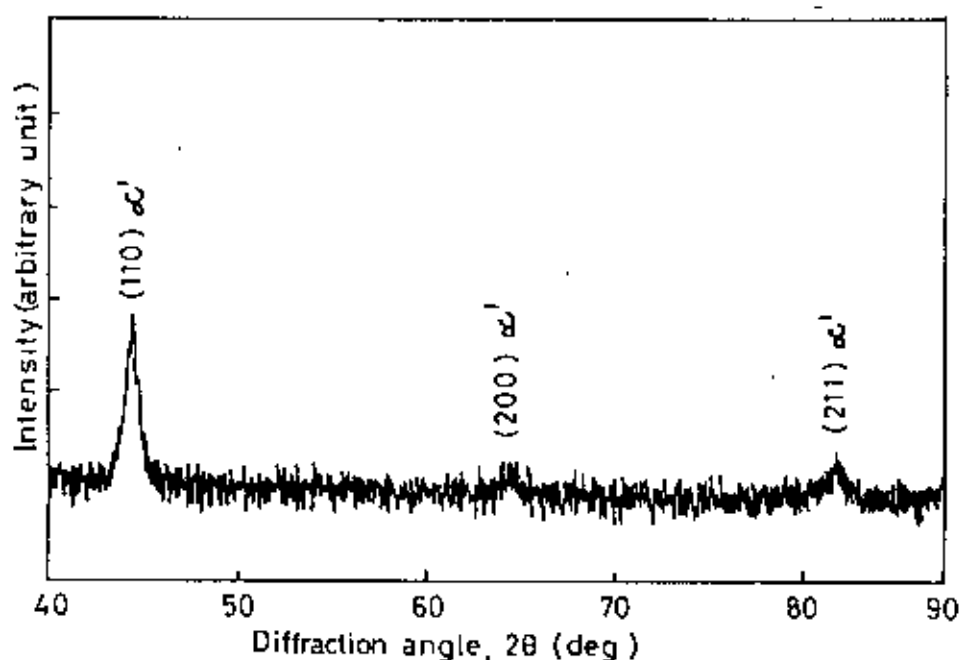


Fig. 4.7 X-ray diffraction pattern of as-deposited Fe-1.1%C alloy.
(Current density: 40 mA/cm^2 , Deposition time: 1 hr.)

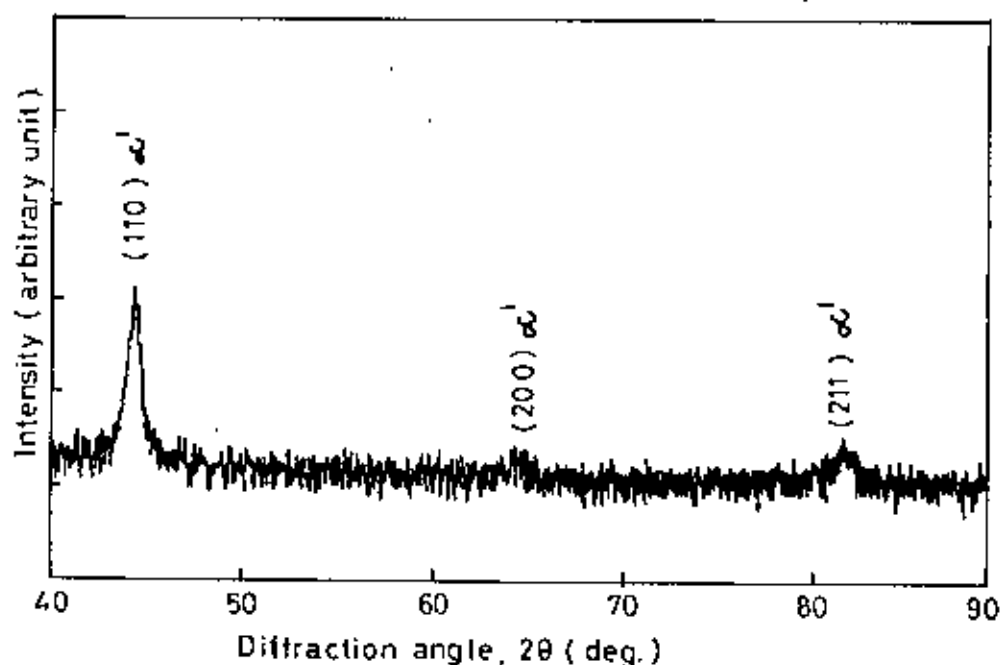


Fig. 4.8 X-ray diffraction pattern of tempered Fe-1.1%C alloy.
(Current density: 40 mA/cm^2 , Deposition time: 1 hr.)

4.1.4. Differential thermal analysis

Fig. 4.9 and 4.10 shows the DTA curves of as-deposited Fe-1.1%C alloy and annealed commercial file steel respectively. As the deposit possesses about 1.1% carbon, compositionally it is similar to file steel. However, the DTA curve of electrodeposited iron-carbon alloy is seen to be different from that of annealed file steel. The DTA curve of as-deposited Fe-C alloy shows a number of extra peaks compared to file steel.

Iron-carbon alloy transforms into gamma iron through eutectoid transformation at 723°C during slow heating. Eutectoid transformation of alpha iron into gamma iron involves an enthalpy change of $\Delta H = +875 \text{ cal/mole}^{62}$ and hence the reaction is endothermic. Relatively rapid cooling may raise the eutectoid transformation temperature to a higher value. Therefore the exothermic peak at about 760°C in both cases is thought to be related to the eutectoid transformation. The martensitic structure of as-deposited Fe-1.1%C alloy has been confirmed by Izaki and Enomoto⁶ by transmission electron microscope and by X-ray diffraction method. Therefore, the presence of extra peaks at 310°C ,

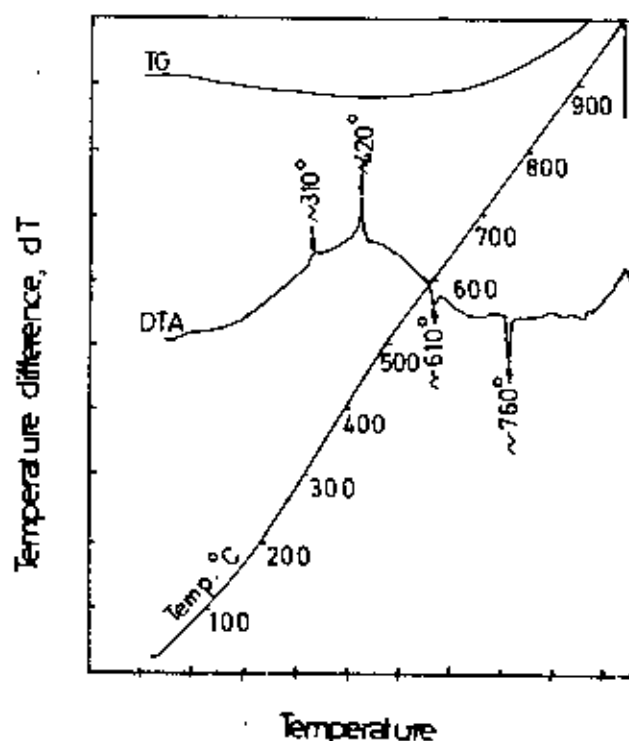


Fig. 4.9 Differential thermal analysis curve of as-deposited Fe-1.1%C alloy.

420⁰C and 610⁰C in the DTA curve of as-plated iron-carbon alloy is probably related to the transformation of martensitic structure of the sample. These peaks are believed to arise during heating due to the transformation of martensite into more stable phases. The transformation of as-deposited Fe-1.1%C alloy into cementite and pearlite phases is also observed in the present study when annealed at 850⁰C for 25 min.

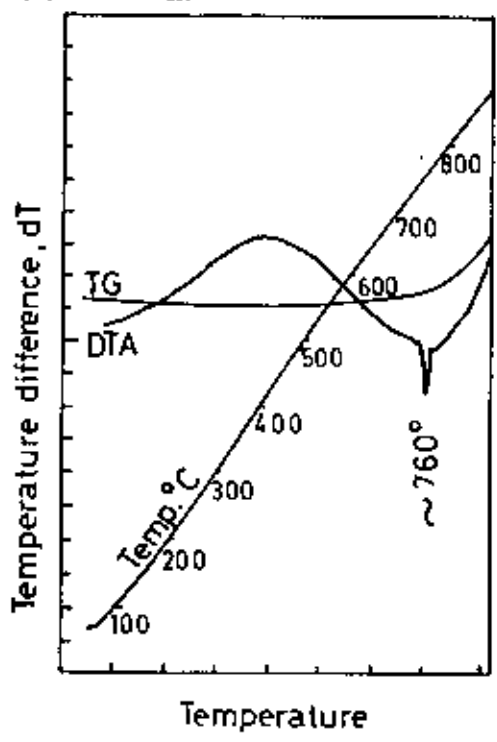


Fig. 4.10 Differential thermal analysis curve of annealed file steel.

4.2 Properties of Fe-C and Fe-Ni-C alloy coatings

4.2.1 Hardness

Fig. 4.11 shows the variation in microhardness of Fe-1.1%C alloy deposited from baths containing various amount of CA and LAA. Microhardness of pure iron coating deposited from CA and LAA free bath is also shown for comparison. Deposits from bath containing 10 g/l CA and 10 g/l LAA with a carbon content of about 1.1 wt% shows maximum hardness of 790 HV. Hardness values of deposits from baths containing (1.5 g/l CA + 1.5 g/l LAA) and (0.5 g/l CA + 0.5 g/l LAA) are 701 and 386 HV respectively. Although the hardness of iron-carbon deposits is consistent with the fact that hardness decreases with a decrease in carbon content (compare Fig. 4.1 and Fig. 4.11), the hardness of the deposit containing 0.88%C (deposited from 0.5 g/l CA + 0.5 g/l LAA) is disproportionately too low. Hardness of the latter deposit is a little higher than

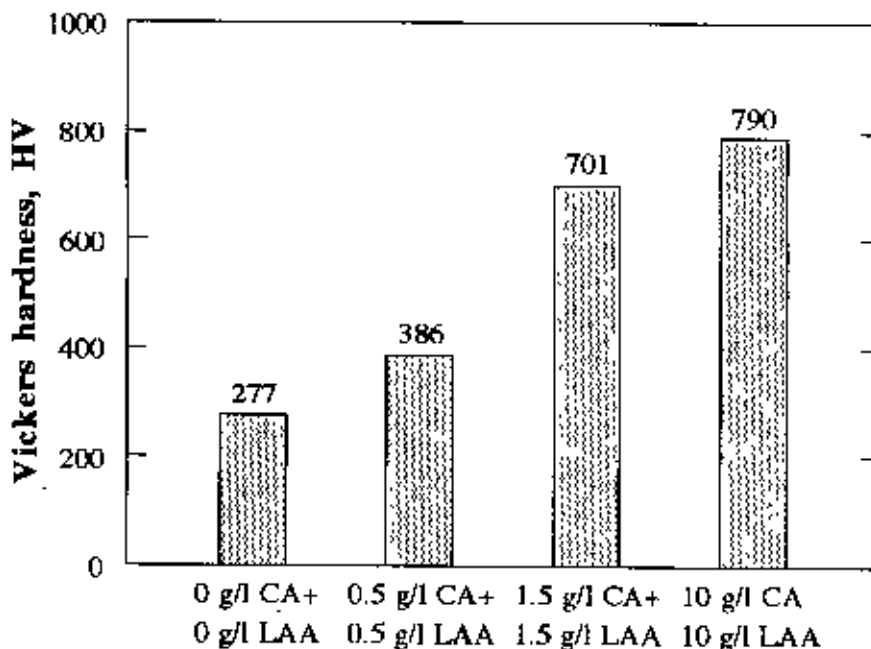


Fig. 4.11 Microhardness of Fe-C alloys deposited from baths containing 150 g/l ferrous sulphate and varying amount of citric acid (CA) and L-ascorbic acid (LAA).

that of pure iron coating. High hardness coupled with high carbon content of iron-carbon deposits from baths B and C suggests the deposits to be of the martensitic type. This fact has already been substantiated by others^{6,8}. The Fe-0.88%C deposit from bath D possesses too low a hardness (386 HV) to be martensitic⁶³. Detailed investigation is necessary to elucidate the structure of this deposit.

The microhardness of as-deposited Fe-1.1%C alloy and Fe-4.3%Ni-1.1%C alloy is compared in Fig. 4.12. Hardness of pure iron is also shown in the figure. Both Fe-1.1%C and Fe-4.3%Ni-1.1%C alloy show higher hardness than pure iron. But Fe-4.3%Ni-1.1%C alloy shows a slightly lower hardness than Fe-1.1%C alloy. It is to be noted that both Fe-1.1%C alloy (Bath B) and Fe-4.3%Ni-1.1%C alloy (Bath F) possess about the same carbon content (Fig. 4.2). As nickel does not show any negative effect on hardness of steel⁶⁴, causes of this decrease in hardness is not clear at present. It can perhaps be related to experimental variation.

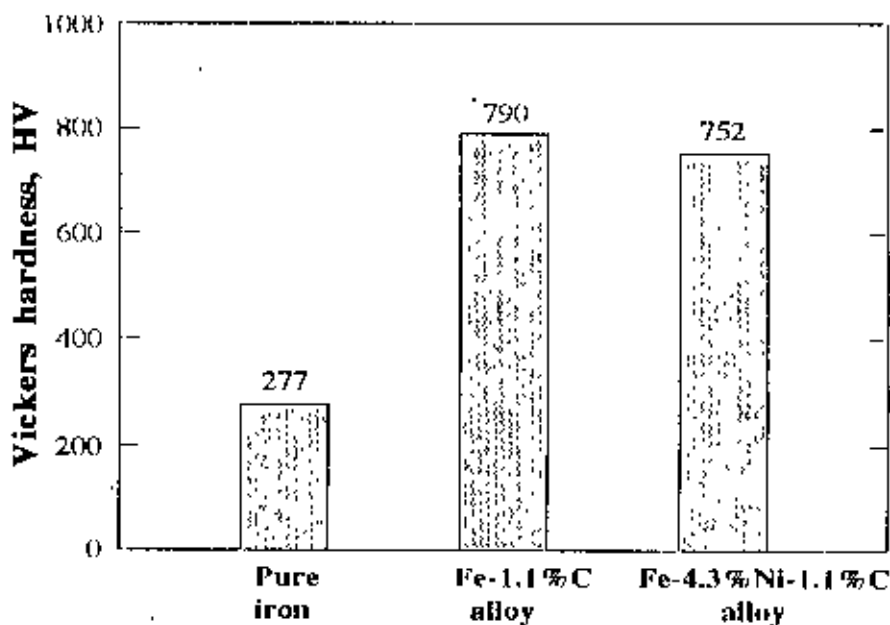


Fig. 4.12 Comparison of microhardness of pure iron, Fe-1.1%C alloy and Fe-4.3%Ni-1.1%C alloy deposited from bath A, bath B and bath F respectively.

The effect of the addition of gelatin to plating bath on the microhardness of iron-carbon alloy coating is shown in Fig. 4.13. According to the figure, as the amount of gelatin in the bath increases, the hardness of the iron-carbon alloy deposit linearly decreases. This decreasing tendency of hardness of the deposit may be due to a number of reasons such as low carbon content, poor morphology, low residual stresses etc. However, by chemical analysis the carbon content of the deposit from bath containing 0.2 g/l gelatin is found to be about 1.55 wt%. The morphology of these deposits is rough compared to Fe-1.1%C and Fe-4.3%Ni-1.1%C alloy deposit as given in Fig. 4.5. It has been found⁸ that deposits with rough morphology may cause mechanical entrapment of carbon at crevices in addition to carbon being incorporated into iron lattice. In such cases overall carbon content may show a high value, although actual carbon percentage included in iron lattices may be lower. Consequently hardness of such deposit may show a lower value. In the present case, low carbon content of the lattice, rough morphology and lower stressed condition of the deposit in presence of gelatin may combinidly have caused the low hardness of the deposit.

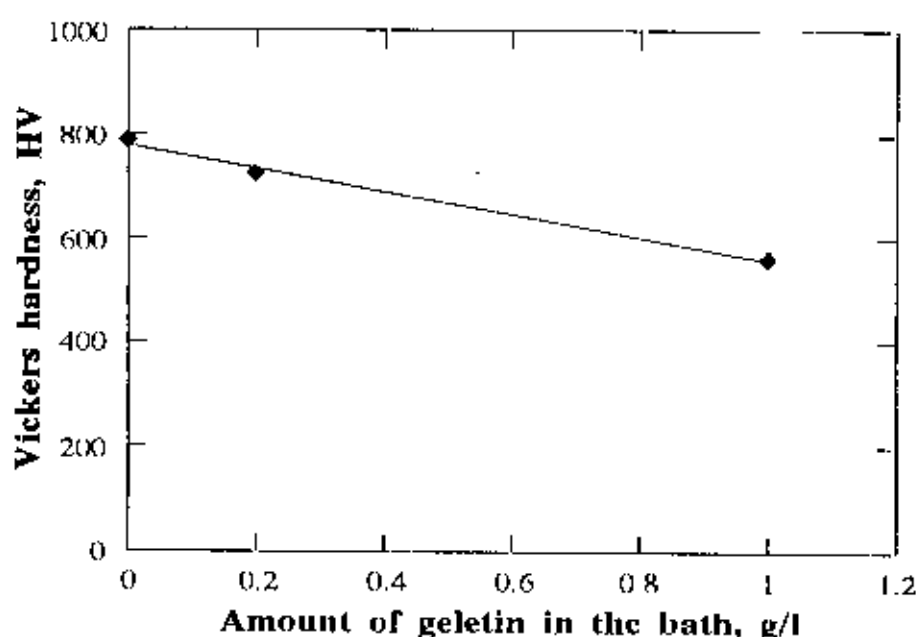


Fig. 4.13 Microhardness of Fe-C alloy deposited from baths containing 150 g/l $FeSO_4$, 10 g/l citric acid (CA) and 10 g/l L-ascorbic acid (LAA) and varying amount of gelatin.

4.2.2 Ductility

Improvement of ductility of iron-carbon alloy was one of the objectives in this study and therefore a number of samples were subjected to bend test following the ASTM B 489-68 Standard⁴⁸.

The ductility of Fe-1.1%C coating in the as-deposited and tempered condition is compared in Fig. 4.14. Spread of the values of percentage elongation as obtained from bend tests is shown by error bar. A slight improvement in elongation from 4% in the as-deposited condition to 5.45% has occurred due to tempering at 200⁰C for 0.5 hour. Heating after plating at relatively low temperature e.g. 100 to 200⁰C occasionally can improve adhesion⁵⁹ and therefore, the ductility raises to a higher value as the deposits are attached to their substrates⁶⁵. Again, it is well known that upon tempering of iron-carbon based alloys at temperature up to 250⁰C, precipitation of epsilon carbide and a slight loss of tetragonality of martensite occur⁵⁶. This is termed as the first stage of tempering. Tempering conditions used in the present study belongs to this first stage. Since no major

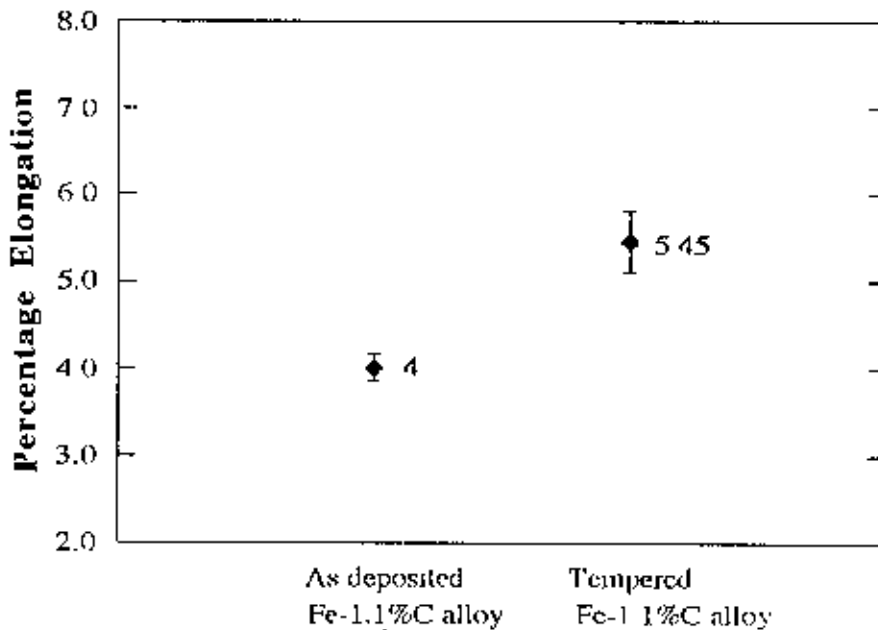


Fig. 4.14 Effect of tempering on the ductility of as deposited Fe-1.1%C alloy coating.

structural changes occur in this stage, the marginal increase in elongation obtained in the present case is therefore expected. In fact the hardness of the deposit was found to be as high as 766 HV after tempering as compared with as-deposited hardness of 790 HV. Tempering also causes loss of residual or intrinsic stresses of as-deposited martensitic Fe-1.1%C alloy and this may be a probable reason for the slight decrease in hardness of the deposit.

The ductility of Fe-4.3%Ni-1.1%C alloy is compared with that of Fe-1.1%C deposit in Fig. 4.15. The percentage elongation of the as-deposited Fe-4.3%Ni-1.1%C alloy is found to be almost double the elongation value of as-deposited Fe-1.1%C deposit. It may be mentioned that Fe-4.3%Ni-1.1%C alloy had a hardness of 752 and 700 HV in the as-deposited and tempered conditions respectively. Effect of nickel on the properties of steel is described in the literature^{56,66}. Nickel has been found to toughen and strengthen steels. Since nickel raises the stacking fault energy, it reduces the extent of work hardening thus resulting in greater deformation prior to fracture. Therefore, improved ductility caused by the incorporation of nickel into electrodeposited iron-carbon alloy is consistent with earlier studies on thermally prepared alloys. However, tempering of Fe-4.3%Ni-1.1%C did not show any improvement in percentage elongation over the value in the as-deposited condition.

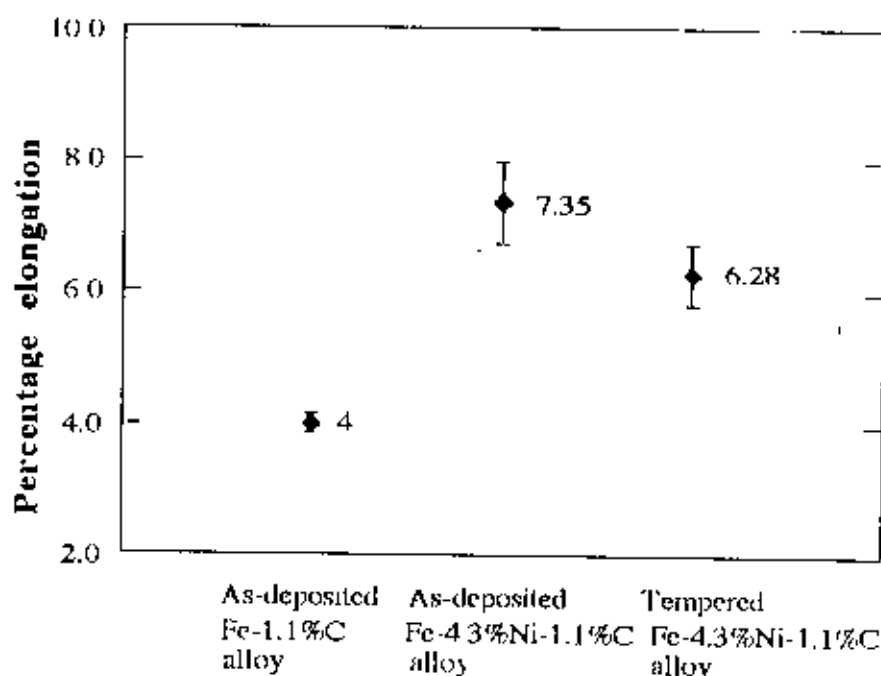


Fig. 4.15 Variation in ductility of the Fe-4.3%Ni-1.1%C alloy deposit. Ductility of Fe-1.1%C alloy deposit is shown for comparison.

The effect of gelatin (0.2 g/l) on the ductility of as-deposited and tempered Fe-1.55%C alloy is presented in Fig. 4.16. According to the figure addition of gelatin in the bath improves ductility of the Fe-1.1%C deposit. Upon tempering the ductility is further improved, even more than as-deposited Fe-4.3%Ni-1.1%C alloy. Although chemical analysis shows high carbon content of the deposit, but it plays no detrimental effect on ductility, because all the carbon is probably not incorporated into the lattice, some might have been entrapped on the surface mechanically⁸. Gelatin is generally known to refine grains, produce compact deposit and suppress dendritic growth⁶⁰. All these factors can lead to improved ductility of the coating. However, the actual mechanism by which gelatin causes an improvement of ductility of iron-carbon deposits needs further investigation.

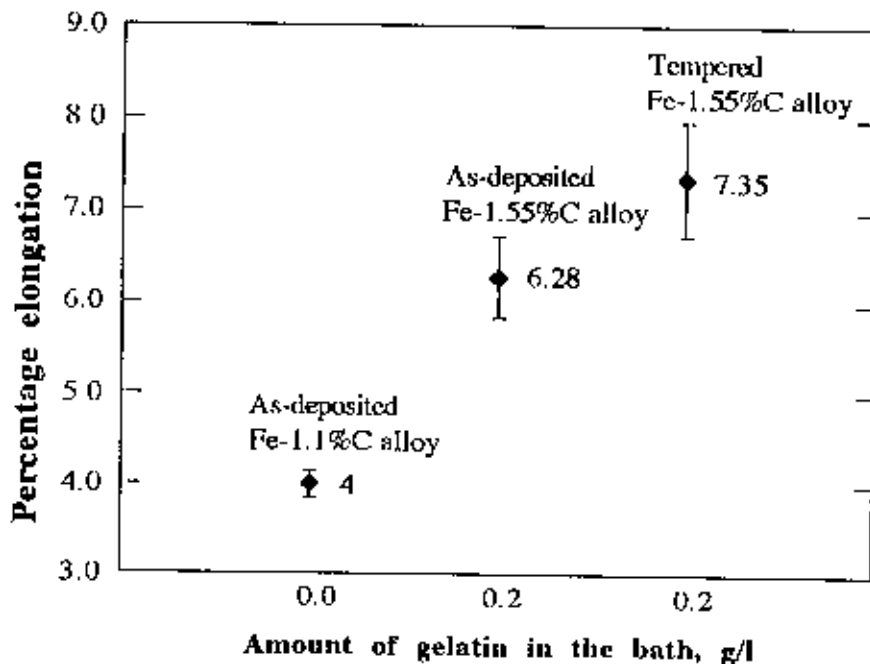


Fig. 4.16 Variation in ductility of the Fe-1.55%C alloy deposits obtained from bath containing gelatin as additive.

4.2.3 Wear properties

In a previous study⁶⁷, the extent of wear damage on electroplated pin was expressed by the width of the scar on the pin. In the present work, wear scar width has been also used to measure the extent of wear damage. Fig. 4.17 shows the variation in the width of wear scar on Fe-1.1%C alloy coated mild steel pin as a function of sliding distance. The samples were tested in the as-deposited condition under a constant load of 250 g. That extent of wear damage increases with sliding distance is clearly evident from increased width of the scar.

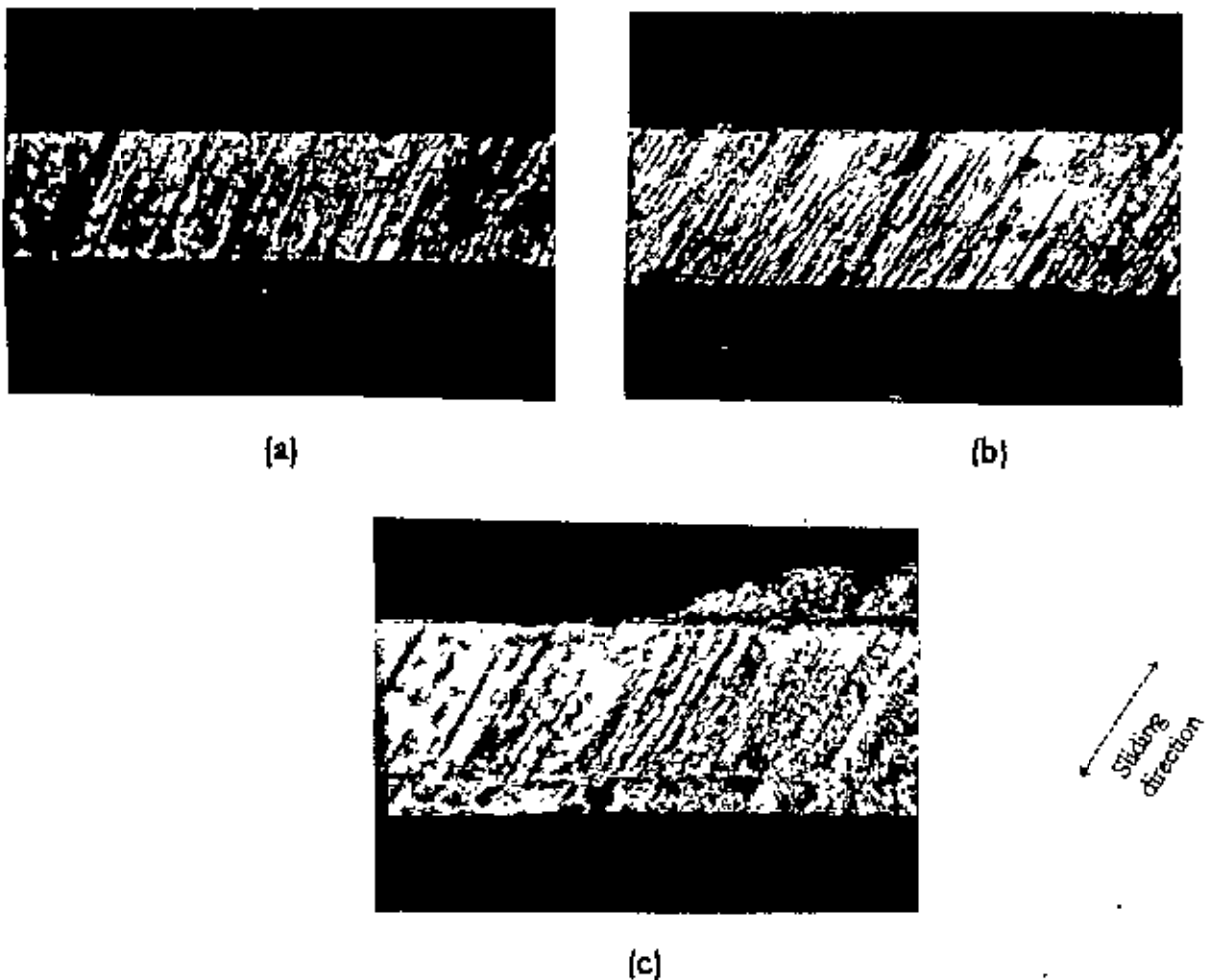


Fig. 4.17 Macrographs of wear scar on as-deposited Fe-1.1 wt%C alloy coating on mild steel pin subjected to wear at a constant load of 250 g.

- a) Sliding distance, 416 m.
- b) Sliding distance, 832 m.
- c) Sliding distance, 1248 m.

Width of wear scar on as-deposited and tempered Fe-1.1%C alloy coated pin and bare mild steel pin tested under a load of 250 g is shown as a function of sliding distance in Fig. 4.18. The wear scar width of as deposited Fe-1.1%C alloy increases rather sharply at the beginning. The increase becomes more gradual at longer sliding distance. The as-deposited Fe-1.1%C alloy is found to suffer most from wear damage. Extent of wear damage on mild steel is seen to be the lowest.

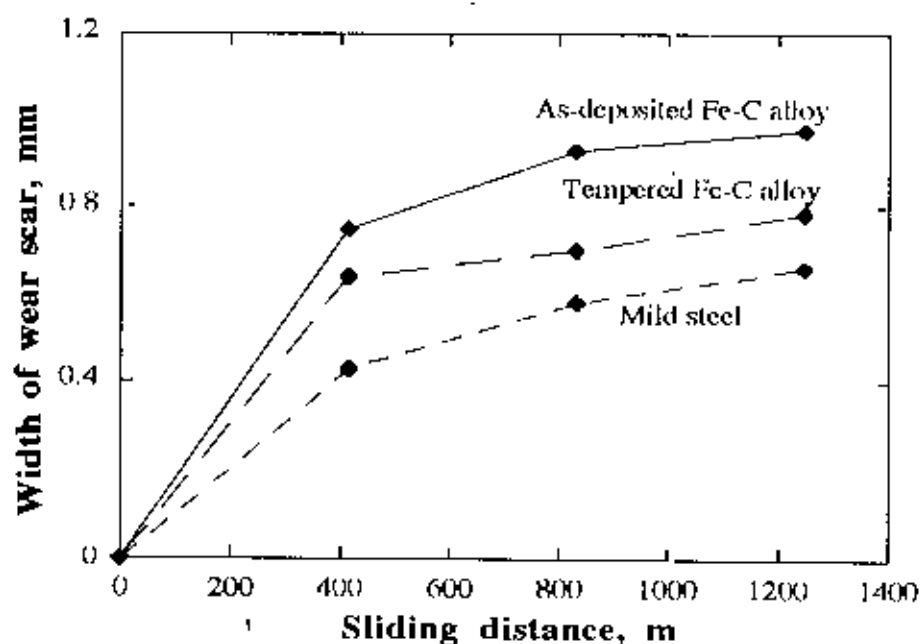


Fig. 4.18 Variation in wear scar on as-deposited Fe-1.1 wt%C alloy pin, tempered Fe- 1.1 wt%C alloy pin and mild steel pin as a function of sliding distance at an applied load of 250 g.

Fig. 4.19 shows the width of the wear scar on as-deposited and tempered Fe-1.1%C alloy and mild steel at two different sliding distances at an applied load of 500 g. According to the figure it is apparent that increasing sliding distance increases wear of all the samples. Mild steel is found to be the most resistant to wear among the three samples. This was also observed when the samples were tested at a load of 250 g. However, the tempered Fe-1.1%C alloy shows anomalous behaviour when tested under 500 g load. It seems to exhibit wear

resistance lower than that of as-deposited coating. Under 500 g load, tests for longer sliding distance cause complete wear of the coating and exposure of the substrate. Under 1000 g load, substrate of tempered Fe-1.1%C alloy is exposed even at low (416 m) sliding distance, whereas as-deposited Fe-1.1%C does not show such behaviour. So, it is apparent from this study that, at higher loads and sliding distances tempered Fe-1.1%C alloy deposit shows poor wear resistance than as-deposited Fe-1.1%C alloy.

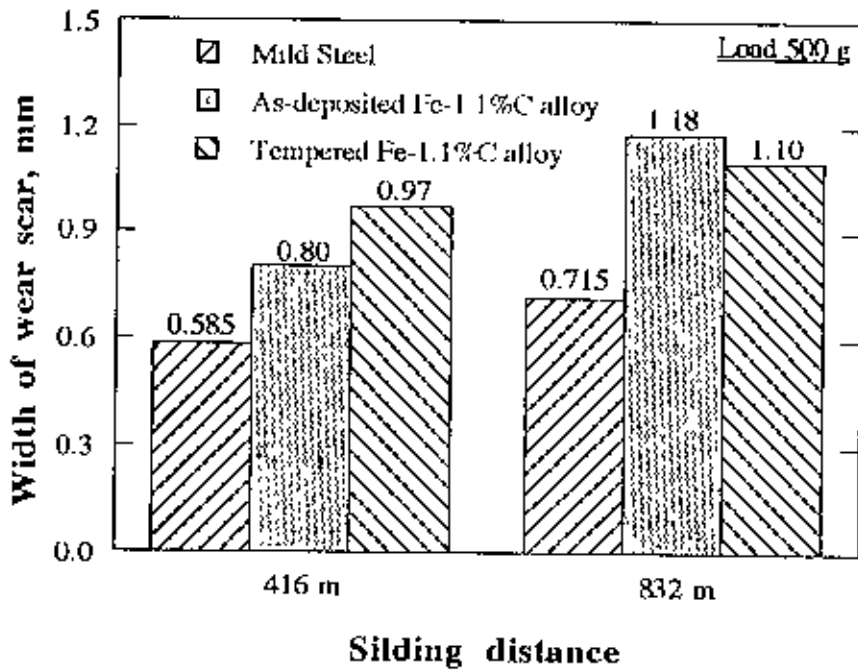
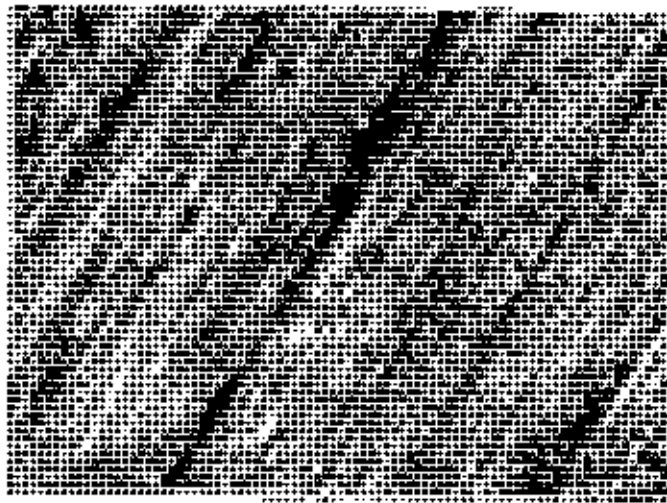
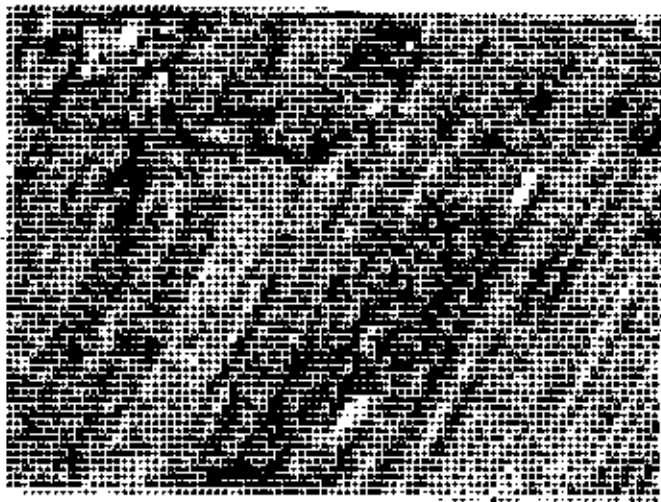


Fig. 4.19 Variation in wear scar of mild steel, as-deposited Fe-1.1%C alloy and tempered Fe-1.1%C alloy as a function of sliding distance at constant load of 500 g.

The micrographs of Fig. 4.20 illustrate the appearance of the worn surface of as-deposited Fe-1.1%C alloy with different load but at constant sliding distances. Scars are characterised mainly by fine sliding marks. These sliding marks indicate that abrasive wear has taken place during testing. In addition, presence of dark patches of smeared transfer layer is also visible in the micrographs. The latter feature is indicative of adhesive type of wear. It is concluded that although abrasive wear is the main mechanism on Fe-1.1%C alloy coated pin, adhesive wear is also operative to some extent.



(a)



(b)

Fig. 4.20 Micrograph of wear scar on as-deposited Fe-1.1%C alloy coating.

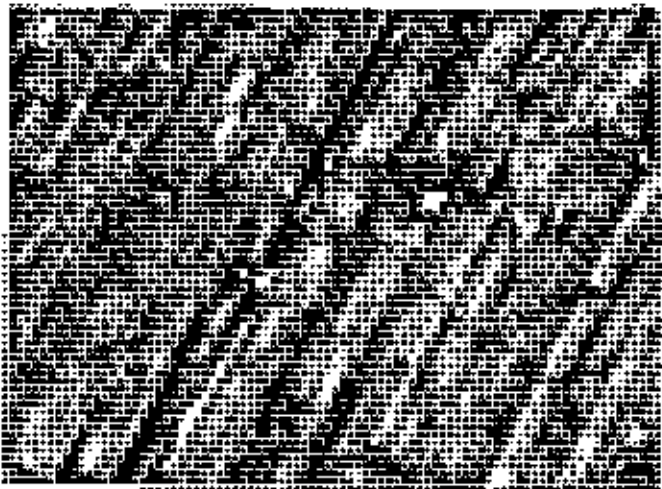
a) Sliding distance 416 m, load 250 g.

b) Sliding distance 416 m, load 500 g.

The micrographs of worn surfaces of tempered Fe-1.1%C alloy are shown in Fig. 4.21. The scar nature and appearance are similar to as-deposited Fe-1.1%C alloy. The fine scratches in the sliding direction is most probably due to the abrasive wear arising from movement of wear debris between the pin and the disc. The micrographs also show the network of fine hair-line cracks that formed during tempering. These cracks may aid lubricant retention as in hard chrome plating.



(a)



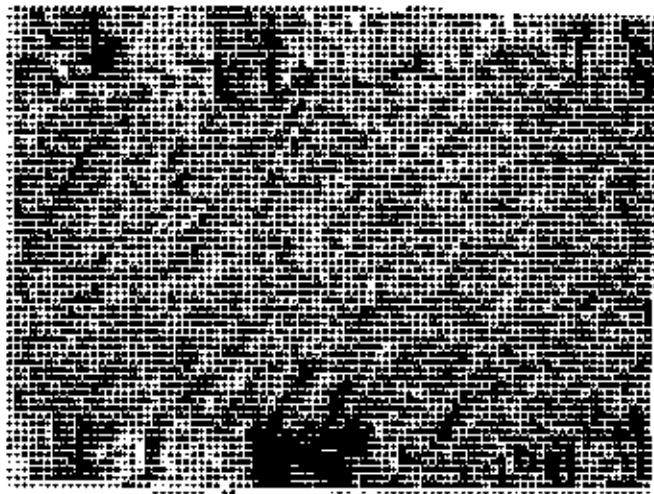
(b)

Fig. 4.21 Micrograph of wear scar on tempered Fe-1.1%C alloy coating.

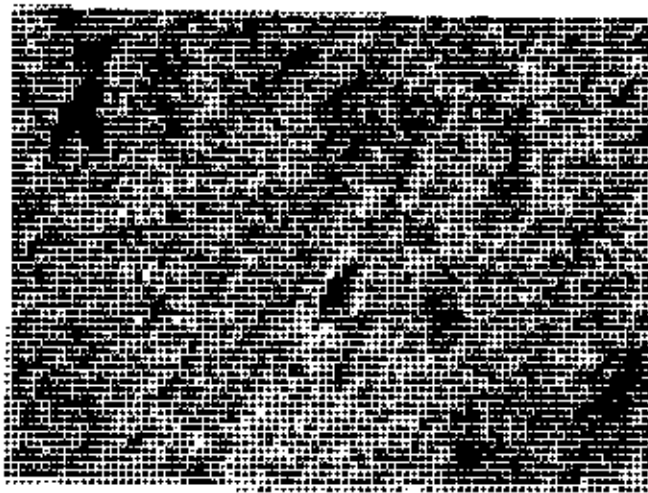
a) Sliding distance 416 m, load 250 g.

b) Sliding distance 416 m, load 500 g.

Fig. 4.22 shows the micrograph of worn surfaces of mild steel at different loads and sliding distances. Scars on the samples are not smooth, and edges are found to be irregular. Plastic flow of materials was observed along the sliding direction at the exit edge of the scar. The sliding marks on the scar are uneven and ill defined. Wide spread presence of transfer layer is observed. All these suggest that adhesive wear is the predominant mechanism in the case of mild steel pin.



(a)



(b)

Fig. 4.22 Micrograph of wear scar on mild steel.

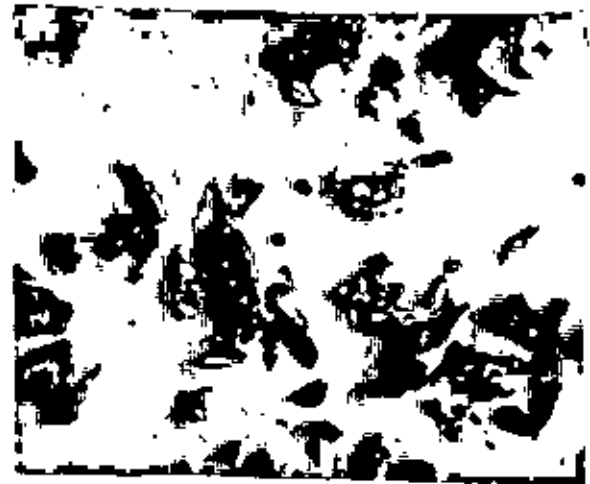
a) Sliding distance 416 m, load 250 g.

b) Sliding distance 416 m, load 1000 g.

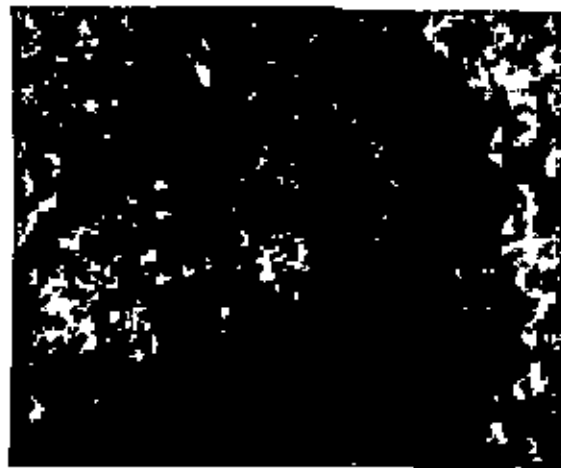
The macrographs of debris of as-deposited Fe-1.1%C alloy, tempered Fe-1.1%C alloy and mild steel are shown in Fig. 4.23. In the case of Fe-1.1%C alloy coatings, both in the as-deposited and hardened conditions, the wear debris is found to be rather large. They show metallic lustre at the broken face. Such debris seems to have generated through brittle fracture. On the other hand, debris generated during the wear test of bare mild steel pin is fine and powdery. The debris in this case is found to consist of dark oxidised particles.



(a)



(b)



(c)

Fig. 4.23 Macrographs of wear debris collected during wear testing.

- a) As-deposited Fe-C alloy
- b) Tempered Fe-C alloy
- c) Mild steel

Welsh⁵², Sexton and Fischer⁵³ have shown that in the case of mild wear fine, oxidised debris is formed. Whereas, flaky, large particles are generated as debris when wear is of the severe type. This is found to be consistent with the present experimental data. Mild steel pin with fine powdery debris is observed to suffer least due to wear while the wear damage is much more severe on iron-carbon coating.

Archard equation is commonly used to express wear rate as a function of test variables and hardness of the material⁶⁸. The equation is written as,

$$\text{Time rate of wear, } \eta = K_{\alpha} WV/H$$

- where, W = Applied load
 V = Sliding speed
 H = Hardness of the material
 K_{α} = Wear coefficient.

According to Archard equation, Fe-1.1%C coatings having higher hardness should be more wear resistant than mild steel with lower hardness of about 238 HV. However, the opposite has been observed in the present study. It is thought that not only hardness but also toughness plays a significant role in wear. Thus iron-carbon coating with low toughness fails in a brittle manner and undergoes severe wear. Other properties of the coating like its adherence with substrate etc. can also play a vital role. In depth study is necessary to find out the exact causes of enhanced wear of iron-carbon coatings and ways to improve their wear resistance.

5. CONCLUSIONS

The following conclusions can be drawn from this study:

1. Martensitic iron-carbon alloy with carbon content of 1.1 wt% and hardness as high as 790 HV can be obtained by electrodeposition at room temperature from ferrous sulphate bath containing 10 g/l citric acid and 10 g/l L-ascorbic acid.
2. It is observed that the carbon content of the Fe-C deposits becomes less sensitive to CA and LAA content of the bath as higher amounts of CA and LAA are added.
3. Presence of nickel sulphate in the bath does not affect the carbon content of the Fe-C alloy deposit to any appreciable extent. It has been possible to deposit Fe-4.3%Ni-1.1%C alloy coating with a hardness of 752 HV from bath containing iron sulphate and nickel sulphate and 10 g/l each of citric acid and L-ascorbic acid.
4. As the amount of citric acid and L-ascorbic acid in the bath decreases, the corresponding hardness of the deposit also decreases. Presence of gelatin in the bath decreases the hardness of the deposit.
5. Tempered Fe-1.1%C alloy deposit obtained by electrodeposition shows higher ductility than as-deposited Fe-1.1%C alloy. Electrodeposited Fe-4.3%Ni-1.1%C alloy possesses better ductility than as deposited and tempered Fe-1.1%C alloy. Fe-1.1%C alloy deposited from bath containing 0.2 g/l gelatin exhibits maximum ductility.
6. In spite of high hardness, Fe-1.1%C alloy coatings is found to possess wear resistance lower than that of mild steel probably due to their low toughness and insufficient adhesion.

6. SUGGESTIONS FOR FUTURE STUDY

1. The present bath composition should be modified to obtain a Fe-C alloy deposit with better mechanical properties. Particularly, attempt should be made to improve the ductility of the Fe-C alloy by adding stress relieving additive e.g., saccharine in the bath.
2. The structure of as-deposited Fe-C alloy should be investigated by using a Transmission Electron Microscope.
3. Attempts should be made to understand the wear behaviour of Fe-C alloy coatings. Measures should be taken to improve the adhesion of Fe-C alloy coating to substrate. This is expected to lead to better wear resistance.
4. The wear resistance of Fe-Ni-C alloy should also be investigated.

7. REFERENCES

1. T. Omi, H. L. Glass, and H. Yamamoto, Phase structure and composition of Fe-W alloy electrodeposits, *J. Electrochem. Soc. Electrochemical Science and Technology*, 123, (1976), 341-348.
2. S. W. Yao, H. T. Guo, C. Wang and M. Kowaka., Amorphous Fe-W film electrodeposited by using Fe^{+3} ions, *Mater. Prot (China)*, 25(5), 1992, 9-12.
3. Y. P. Lu, Z. Y. Yi and J. X. Wu. Effect of saccharine on electrodeposition of Fe-Cr-Ni alloys, *Mater. Prot. (China)*, 25(5), (1992), 13-16.
4. M. Kowaka, M. Li. (Uyemura), *Hyomen Gijdsu*, Structure of Fe-Ni-W alloy films electrodeposited from organic phosphoric acid baths and their characteristics, (*J. Surf. Finish. Soci. Jpn.*), 44(9), (1993), 748-759.
5. J. Luo, M. Wang, The electrodeposition of amorphous FeNiP alloy films, *J. Univ. Sci. Technol. Beijing*, 12(5), (1990), 491-494.
6. M. Izaki and H. Enomoto, *J. Jpn. Inst. Met.*, 56(6), (1992), 636.
7. *in Techno Japan*, 26(2), (1993), 42.
8. A. S. M. A. Haseeb and M. Z. Huq, Electrochemical preparation of martensitic iron-carbon alloy at room temperature, *Proceedings of IMMM*, Interuational Academic Publishers, (1995), 565-570.
9. A. Brenner, The electrodeposition of Copper-Bismuth Alloys from a Perchlorate Bath, Ph.D Thesis, University of Maryland, 1939.
10. S. G. Clarke, W.N. Bradshaw and E.E. Longhurst, Studies on Brass Plating, *J. Electrodepositors, Tech. Soc.* 19, (1994), 63.
11. H. Kersten and J. Mass, Electrodeposited epsilon-brass, *J. Phys. Chem.* 36, (1932), 2175-2177.

12. W. Blum and H. E. Haring, The electrodeposition of lead-tin alloys. *Trans. Am. Electrochem. Soc.* 40, (1921), 287-304.
13. E. P. Schoch and A. Hirsch, The Electrolytic deposition of nickel-zinc alloys. II. *Tran. Am. Electrochem. Soc.* 11, (1907), 135-152.
14. F. Jepson, S. Meecham, and F. W. Salt, The electrodeposition of iron-zinc alloys, *Trans. Inst. Metal Finishing* 32, (1955), 160-180.
15. C. B. F. Young and C. Struyk, Deposition of nickel-cobalt alloys from chloride solutions, *Trans. Electrochem. Soc.* 89, (1946), 383-412.
16. S. Glasstone and J. C. Speakman, The electrodeposition of cobalt-nickel alloys, I. *Trans. Farady Soc.* 26, (1930), 565-574.
17. C. G. Fink and K. h. Lah, The deposition of nickel-cobalt alloys, *Trans. Am. Electrochem. Soc.* 27, (1931), 29-35.
18. S. Glasstone and J. C. Speakman, The electrodeposition of cobalt-nickel alloys. II, *Trans. Farady Soc.* 27, (1931), 29-35.
19. S. Glasstone and T. E. Symes, The electrodeposition of iron-nickel alloys I, *Trans. Farady Soc.* 23, (1931), 213-226.
20. E. Raub, Der Einfluss von Zusätzen Zu Nickelbädern auf die Schädlichkeit des Eisens. *Mitt. Forschungsinst. u. Probieramts Edelmetalle staatl. u. Probieramts Edelmetalle staatl. höheren Fachschule Schwab, Gmünd*, 9, (1935), 1-8.
21. Von Escher, F. Foerster, Tenne. F. Herrschel, M. Schade, and Über Passivitäts-und Verzögerungserscheinungen bei anodischer Entladung der Halogenionen und bei Kathodischer Entladung der Ionen der Eisen metalle, *Z. Elektrochem*, 22, (1916), 85-102.
22. B. Lustman, Study of the deposition potentials and microstructures of electrodeposited nickel-zinc alloys, *Trans. Electrochem. Soc.* 84, (1943), 363-375.

23. C. G. Fink. and C. B. F. Young, Cadmium-zinc alloy plating from acid sulfate solutions, *Trans. Electrochem. Soc.* 67, (1935), 311-336.
24. A. H. Du Rose, The protective value of lead and lead-tin deposits on steel, *Trans. Electrochem. Soc.* 89, (1946), 417-428.
25. B. Lustman, Study of the deposition potentials and microstructures of electrodeposited nickel-zinc alloys, *Trans. Electrochem. Soc.* 84, (1943), 363-375.
26. C. L. Faust, D. J. Henry, and W.G. France, The behaviour of alloy anodes in deposition of silver-cadmium alloys from cyanide baths, *Trans. Electrochem. Soc.* 72, (1937), 479-499.
27. E. Raub and A. Engel, Der Aufbau galvanischer Legierungsniederschläge.III. Die Kupfer-Blei-und Silber-Wismut-Legierungen, *Z. Metallk.* 41, (1950), 485-491.
28. H. Nakamura, X-ray analysis of electrolytic brass, *Soc. Papers Inst. Phys. Chem. Research (Tokyo)* 2, (1925), 287-292.
29. A. Roux and J. Cournot, Etude cristallographique par rayons x de la structure de dépôts électrolytiques simultanés de deux métaux, *Compt. rend. acad. Sc.* 186, (1938), 1733-1736.
30. A. Roux and J. Cournot, Sur quelques résultats d'essais cristallographiques par rayons x, *Rev. met.* 26, (1929), 655-661.
31. H. P. Rooksby, The X-ray structure of speculum electrodeposits, *J. Electrodepositors, Tech. Soc.* 26, (1950), 119-124.
32. E. Raub, Über die Struktur galvanisch abgeschiedener Metalle und Legierungen. *Z. Elektrochem.* 55, (1951), 146-151.
33. A. Brenner, P. Burkhead, and E. Seegmiller, Electrodeposition of tungsten alloys containing iron, nickel, and cobalt, *Research Natl. Bur. Standards* 39, (1947), 351-383.

34. A. Brenner, D.E. Couch, and E.K. Williams, Electrodeposition of alloys of phosphorous with nickel or cobalt, *Research Natl. Bur. Standards* 44, (1950), 109-122.
35. E. Raub, *Galvanische Legierungsniederschläge Methoden berflache*, 7A, (1950), 109-122.
36. K. Aotani, Studies on the electrodeposited alloys, Part 8, On the microscopic structures of electrodeposited alloys, *J. Electrochem. Soc. Japan* 21, (1953), 180-183.
37. K. Aotani, Studies on the electrodeposited alloys, 5. Properties of electrodeposited Ni-Fe alloys, *J. Electrochem. Soc. Japan*. 20, (1952), 88-91.
38. V. Dehlinger and F. Giesen, *Über den Zusammenhang Zwischen regelmässiger Atom-Verteilung and Resistenzgrenzen*, *Z. Metallk.*, 24, (1932), 197-198.
39. V. Montoro, Contribution to the study of electrodeposition of alloys, The constitution of the products. *Met. ital.* 40, (1948), 9-12.
40. V. Montoro, Contributions to the study of the electrodeposition of alloys. II The constitution of the products, *Met. ital.* 41, (1949), 279-286.
41. E. Raub, *Silber-Blei-Legierungen als Gleitlagerwerkstoffe*, *Z. Metallk.* 40, (1949), 167-170.
42. Ye. Xingpu, Ductility of thin electrodeposited copper coatings, Ph.D. Thesis, Faculty of Engg., Katholieke University of Leuven, Belgium, 1990.
43. T. D. Dudderar and F. B. Koch, Mechanical Property Measurements on Electrodeposited Metal Foils, in *Properties of Electrodeposits, Their Measurement and Significance*, R Sard Ed., The Electrochemical Soc., Princetone, New Jersey, (1975), 187-213.
44. M. Pareute and R. Weil, Tensile testing of electrodeposits, *Plating and Surface Finishing*, 71(5), (1984), 114-117.

45. V. A. Lamb and D. R. Valentine, Physical and Mechanical Properties of Electrodeposited Copper, I, Literature survey, *Plating*, (1965), 1289-1311.
46. F. W. Verdi and R. L. Tavani, Tensile testing of electrodeposited copper foils in properties of electrodeposits, their measurements and significance,, Eds. R. Sard, H. Leidheiser, and E. Ogburn, The Electrochemical Soc., Inc., Prinetone, New Jersey, (1975), 214-220.
47. I. Kim and R. Weil, Thickness effects on the mechanical properties of electrodeposits, Preprint American Electrochem. Soc. Conf., (1988).
48. Annual Book of ASTM Standards, American Society for Testing Materials, Philadelphia, Part 9, (1979), 311.
49. Z. Marciniak and K. Kuczynski, Limit Strain in the Processes of Stretch forming Sheet Metal, *Int. J. Mech. Sci.* 9, (1967), 609-620.
50. J. T. Burwell, Survey of possible wear mechanisms, *wear*, 1, (1959), 119.
51. Horst Czichos, Importance of properties of solids to friction and wear behaviour, *New directions in lubrication, materials, wear and surface interactions*, Noyes publication.
52. N. C. Welsh, *Philos. Trans. R. Soc. (London) Ser. A257*, (1964), 31.
53. M. D. Sexton and T. E. Fischer, *Wear* 96, (1984), 17.
54. R. S. Fein and T. H. Randall. in: D. Godfrey, *ASLE Trans.* 5, (1962), 57.
55. M. Kerridge, *Proc. Phys. Soc. (London), Sect. B68*, (1955), 400.
56. R. W. K. Honeycombe, *Steels : Microstructure and Properties*, Edward Arnold, London, (1990), 140.
57. B. C. Agarwal and S. P. Jain, *A Text Book of Metallurgical Analysis*, Khanna Publishers, Delhi, (1984), 96.

58. A. Brenner, Electrodeposition of alloys, Volume I, Academic Press, New York (1963).
59. Jack W. Dini, Electrodeposition: The materials science of coatings and substrates, Noyes Publications, New Jersey, (1993).
60. H. Brown, Function and structure of organic additives in electroplating, Udylite Co, Detroit, Michigan (USA), 114-121.
61. S. E. Beacon and B. J. Riley, Tracer follows leveler in electroplating bath, Nucleonics, 18(5), (1960), 82.
62. G. S. Upadhyaya, Problems in metallurgical thermodynamics and kinetics International series in materials science and technology, Vol. 25, Pergamon Press, (1977).
63. G. R. Speich, Trans. AIME, 245, (1963), 2553.
64. Avner, Introduction to physical metallurgy, Second edition, MacGraw Hill International Book Company, New York, (1974).
65. P. Vatakhov and R. Wirl, The effects of substrate attachment on the mechanical properties of electrodeposits, Thin solid films, 169, (1989), 35.
66. F. B. Pickering, in Metallurgical Achievements, Pergamon Press, London, (1965).
67. M. Moniruzzaman, Study of the mechanical properties of electroplated Zn-Ni alloy coating, M.Sc Thesis, Bangladesh Univ. of Engg. and Tech., Bangladesh (1995).
68. Kenneth C. Ludema, Tribology update, The journal of materials science, 10(5), (1988), 517-541.

